Husky Energy

White Rose Extension Project

Underwater Sound Propagation

June 2012

Husky Energy SUNCOR ENERGY nalcor energy

Underwater Sound Propagation Assessment for the Environmental Assessment of the White Rose Extension Project

Submitted to:
Stantec Inc.
St. John's, NL

Authors:
Marie-Noël R. Matthews
Mikhail Zykov

JASCO Applied Sciences
Suite 202, 32 Troop Ave.
Dartmouth, NS, B3B 1Z1, Canada
Phone: +1.902.405.3336

2012 June 19
P001162-001

Table of Contents

List of Figures

List of Tables

Executive Summary

JASCO Applied Sciences carried out an underwater sound propagation assessment to estimate distances to sound level thresholds around potential underwater acoustic sources resulting from the Husky Oil Operation Ltd. White Rose Extension Project (WREP). Depending upon the options selected, the different phases of WREP may consist of: the construction of a concrete gravity structure (CGS) at Argentia, NL; the transportation of the CGS from Argentia to the White Rose Field site (Grand Banks, offshore Newfoundland); and drilling from a wellhead platform or subsea drill centre in the White Rose field.

This report presents the assessment of underwater sound fields resulting from dredging and blasting operations at three sites near Argentia Harbour, Placentia Bay, and from dredging, drilling, support vessel, and helicopter operations at the White Rose site. Distances to level thresholds from blasting activities are provided as un-weighted and M-weighted sound exposure levels of 120 to 210 dB re 1 $\mu Pa^2 \cdot s$; distances to level thresholds from all sources (impulsive and continuous) are provided as un-weighted and M-weighted rms sound pressure levels of 120 to 200 dB re 1 µPa.

1.0 Introduction

1.1 Overview

JASCO Applied Sciences (JASCO) conducted an underwater sound propagation assessment for the Environmental Assessment of the Husky Oil Operation Ltd. (Husky) White Rose Extension Project (WREP). Depending upon the options selected, the different phases of WREP may consist of: the construction of a concrete gravity structure (CGS) at Argentia, NL; the transportation of the CGS from Argentia to the White Rose field site (Grand Banks, offshore Newfoundland); and drilling from a wellhead platform (WHP) or subsea drill centre in the White Rose field. The CGS and topsides will be joined in Placentia Bay, NL.

JASCO modelled underwater sound propagation around potential underwater acoustic sources resulting from the WREP, to estimate distances to sound level thresholds. The modelled sources represent: dredging and blasting activities near Argentia Harbour, Placentia Bay; operations that may be required to transport the CGS from the construction site in Argentia; and dredging, drilling, support vessel and helicopter activities at the White Rose Field site. Distances to sound level thresholds were estimated for water temperature profiles representative of months that are the most (February) and least (August) conducive to long-range sound propagation, accounting for source directivity and the range-dependent environmental properties in the area.

This report presents the modelled results in two formats. Tables present maximum and 95 percent distances to sound level thresholds. Sound-field contour maps present the directivity and range to various sound level thresholds. Distances to level thresholds from blasting activities (impulsive sources) are provided as un-weighted and M-weighted sound exposure levels (SELs) of 200 through 120 dB re 1 $\mu Pa^2 \cdot s$. Distances to level thresholds from all sources (impulsive and continuous) are provided as un-weighted and M-weighted root-mean-square sound pressure level (rms SPLs) of 200 through 120 dB re 1 µPa.

1.2 Acoustic Metrics

Underwater sound amplitude is measured in decibels (dB), relative to a standard reference pressure of 1 µPa. The rms SPL is commonly used to evaluate the loudness or effects of continuous noise sources. The rms SPL (dB re 1 µPa, ANSI symbol L_p) is the rms pressure level over the time window, T:

$$L_p = 10 \log_{10} \left(\frac{1}{T} \int_T p^2(t) dt \Big/ p_o^2 \right) \quad (1)$$

where T is the time interval in seconds. The rms SPL can be thought of as a measure of the average pressure or as the "effective" pressure over the duration of an acoustic event. For impulsive noise such as the sound from an explosion, T is the duration of one acoustic pulse. Because T is used as a divisor, pulses that are more spread out in time have a lower rms SPL for the same total acoustic energy.

The SEL (dB re 1 $\mu Pa^2 \cdot s$, ANSI symbol L_E) is also commonly used to quantifying loudness of impulsive sources. It is the time integral of the squared pressure over a fixed-time window containing the entire pulse, T:

$$L_E = 10\log_{10}\left(\int_T p^2(t)dt \Big/ T_o p_o^2\right) \quad (2)$$

where T_o is a reference time interval of 1 s. The per-pulse SEL is measured in units of dB re 1 μPa·√s or equivalently dB re 1 μPa^2·s. This measure represents the total energy delivered over the duration of an acoustic event at a receiver location. The SEL is related to sound energy (or exposure) rather than sound pressure. SEL can be a metric that describes the sound level for a single sound pulse or a cumulative metric, if applied over a period containing multiple pulses.

For continuous sources, *T* is set to 1 s to calculate the rms SPL, making it equivalent to the SEL.

1.3 Acoustic Impact Criteria

1.3.1 Marine Mammal Frequency Weighting

The potential for underwater noise to impact marine species depends on how well the species can hear the sounds produced (Southall et al. 2007). Noises are less likely to disturb or injure animals if they are at frequencies outside the animals' hearing range. For non-injurious sound levels, frequency weighting based on audiograms may be applied to weight the importance of sound levels at particular frequencies in a manner reflective of the receiver's sensitivity to those frequencies (Nedwell and Turnpenny 1998, Nedwell et al. 2007).

Based on a review of literature on marine mammal hearing and on physiological and behavioural responses to anthropogenic sound, Southall et al. (249) proposed standard marine mammal frequency weighting (M-weighting) functions for five functional hearing groups of marine mammals:

- Low-frequency cetaceans (LFCs) - mysticetes (baleen whales)
- Mid-frequency cetaceans (MFCs) - some odontocetes (toothed whales)
- High-frequency cetaceans (HFCs) - odontocetes specialized for using high-frequencies
- Pinnipeds in water - seals, sea lions and walrus
- Pinnipeds in air (not addressed here).

The amount of discount applied by M-weighting functions for less-audible frequencies is lower than that indicated by the corresponding audiograms for member species of these hearing groups. The rationale for applying a smaller discount is due in part to an observed characteristic of mammalian hearing, whereby perceived equal-loudness curves have increasingly less rapid roll-off outside the most sensitive hearing frequency range as sound levels increase. This is the reason that C-weighting curves for humans, used for assessing effects of loud sounds such as blasts, are flatter than A-weighting curves used for quiet to mid-level sounds. Additionally, out-of-band frequencies, although less audible, can still cause physical injury if pressure levels are high enough. Therefore, the M-weighting functions are intended to be applied primarily at high sound levels where impacts such as temporary or permanent hearing threshold shifts may occur. The use of M-weighting should be considered

precautionary (in the sense of overestimating the potential impact), particularly when applied to lower level impacts such as onset of behavioural response. Figure 1-1 shows the decibel frequency weighting of the M-weighting functions for each functional hearing group underwater.

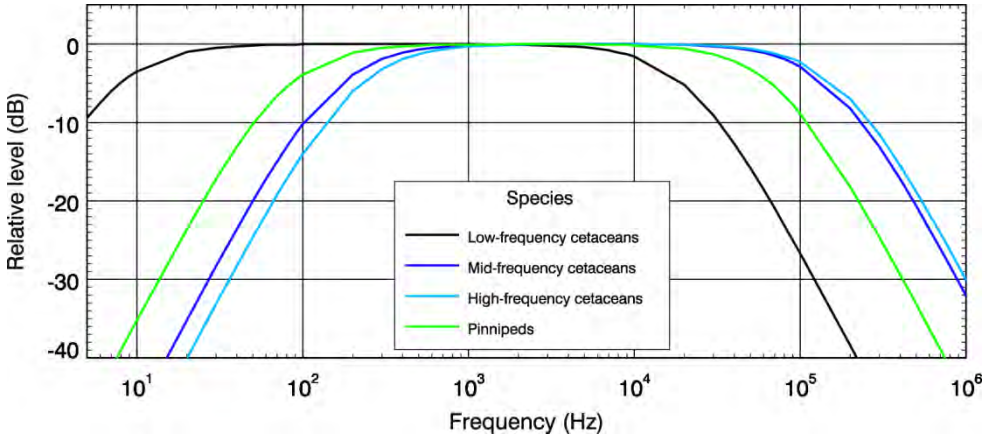

Figure 1-1 Standard M-weighting functions for low-, mid-, and high-frequency cetaceans and for pinnipeds in water

These functions have unity gain (0 dB) through the passband and the high and low frequency roll-offs are approximately −12 dB per octave. The amplitude response of the M-weighting functions is defined in the frequency domain by:

$$G(f) = -20\log_{10}\left[\left(1+\frac{f_{lo}^{2}}{f^{2}}\right)\left(1+\frac{f^{2}}{f_{hi}^{2}}\right)\right] \qquad (3)$$

The roll-off and passband of these functions are controlled by parameters f_{lo} and f_{hi}, estimated upper and lower hearing limits specific to each functional hearing group (Table 1-1).

Table 1-1 Low- and high-frequency cut-off parameters of M-weighting functions for each marine mammal functional hearing group

Functional Hearing group	f_{lo} (Hz)	f_{hi} (Hz)
Low-frequency cetaceans (LFC)	7	22 000
Mid-frequency cetaceans (MFC)	150	160 000
High-frequency cetaceans (HFC)	200	180 000
Pinnipeds (in water)	75	75 000

1.3.2 Exposure Criteria

Canada's received-level standards for potential effects of noise on marine mammals are based on criteria developed by the US National Marine Fisheries Service (NMFS), which proposed values of rms SPL as impact criteria. For impulsive sound sources, a broadband received rms SPL of 160 dB re 1 µPa or greater is estimated to cause disruption of behavioural patterns (i.e., harassment) to marine mammals (Marine Mammal Protection Act [MMPA] 2007). Furthermore, concerns about temporary and/or permanent hearing impairment

to cetaceans exist at a broadband received rms SPL of 180 dB re 1 µPa or greater. This level is higher (190 dB re 1 µPa) for pinnipeds in water (Marine Mammal Protection Act [MMPA] 2007). This harassment criterion (the most cautionary injury impact criterion) was thought to be well understood by the public and easily calculated from standard propagation models (NMFS 2005). Expressed in rms units, the criterion accounts for not only the energy of the pulse, but also the length of the pulse (see Equation 1). The disadvantage of such a criterion is that it does not account for important attributes of exposure such as exposure duration, sound frequency composition and pulse repetition rate. Also, these exposure levels are calculated using un-weighted acoustic signals (i.e., the criterion does not account for the different hearing ability of animals at different frequencies).

1.3.3 Southall Criteria

The Noise Criteria Group, sponsored by NMFS, was established in 2005 to address shortcomings of the 180 to 160 dB re 1 µPa rms SPL criteria. The goals of the Noise Criteria Group were to review literature on marine mammal hearing and marine mammal behavioural and physiological responses to anthropogenic noise, and to propose new noise exposure criteria. In 2007, the findings were published by an assembly of experts (Southall *et al.* 2007). The publication introduced new threshold levels, now commonly referred to as the "Southall criteria".

These so-called "dual-criteria" are based on both zero-to-peak (peak) SPL of acoustic waves, expressed in dB re 1 µPa, and total SEL, expressed in dB re 1 $\mu Pa^2 \cdot s$. A received sound exposure is assumed to cause injury if it exceeds either the peak SPL or SEL criterion, or both. The peak SPL is not frequency weighted, whereas the SEL is M-weighted for the given marine mammal group (see Section 1.3.1).

Different levels were established for cetaceans and pinnipeds, with the levels for pinnipeds being lower than for cetaceans. During the calculations of SEL, the length of the pulse is not considered, only the total energy released during the pulse event (see Equation 2).

Table 1-2 Southall criteria for injury and behavioural disturbance

Marine Mammal Hearing Group	Injury		Behavioural disturbance	
	Peak SPL (dB re 1 µPa)	SEL (dB re 1 $\mu Pa^2 \cdot s$)	Peak SPL (dB re 1 µPa)	SEL (dB re 1 $\mu Pa^2 \cdot s$)
Low-frequency cetaceans (LFC)	230	198 (M_{LFC})	224	183 (M_{LFC})
Mid-frequency cetaceans (MFC)	230	198 (M_{MFC})	224	183 (M_{MFC})
High-frequency cetaceans (HFC)	230	198 (M_{HFC})	224	183 (M_{HFC})
Pinnipeds in water	218	186 (M_{Pinn})	212	171 (M_{Pinn})
Source: Southall *et al.* 2007 Note: The peak SPL criterion is un-weighted (i.e., flat weighted), whereas the SEL criterion is M-weighted for the given marine mammal functional hearing group				

2.0 Methods

The various operations involved in the WREP were divided into nearshore and offshore operations:

- The nearshore operations include blasting and dredging required for transporting the CGS from Argentia Harbour to a mating site in Placentia Bay; and

- The offshore operations include dredging in the White Rose field, drilling at the WHP or subsea drill centre, and the use of a support vessel and a helicopter around the WHP.

Several complementary acoustic models were used to predict the underwater acoustic field associated with the studied operations. First, the source levels representing each operation (or acoustic source) were estimated, either through modelling with Conventional Weapons Effects software (ConWep, v2.0 released August 1992, Hyde 1988) for blasting, or from levels recorded for surrogate sources (Section 2.2). Next, sound was propagated through the underwater environment using one or multiple propagation models (Section 2.3). The choice of propagation model depended mainly on the source's location (in-ground, in-water, or in-air) and its frequency spectrum. Finally, marine mammal frequency weighting (M-weighting; see Section 1.3.1) for four functional hearing groups was applied to weight the importance of received sound levels at particular frequencies.

2.1 Modelled Scenarios

Dredging is planned for three locations near Argentia, Placentia Bay, to facilitate the transportation of the CGS to sea. If the sediment is too hard for suction dredging, blasting may be used. Nearshore dredging operations were modelled at three locations along the CGS tow track (see Figure 2-1). Blasting was modelled on-shore, 50 m from the water line close to Site A (i.e., inside the limits of the proposed construction pit), and at the south end of Corridor 1. Offshore operations were modelled at one site - White Rose field, where the WHP or subsea drill centre will be located (Figure 2-2). The dredging operations, were modelled, as well as various operations associated with the WHP or subsea drill centre itself (drilling, support vessel and helicopter operations).

Nine scenarios were modelled in total (Table 2-1), and each scenario was modelled for the oceanographic regime during two months: February and August (see Section 2.4).

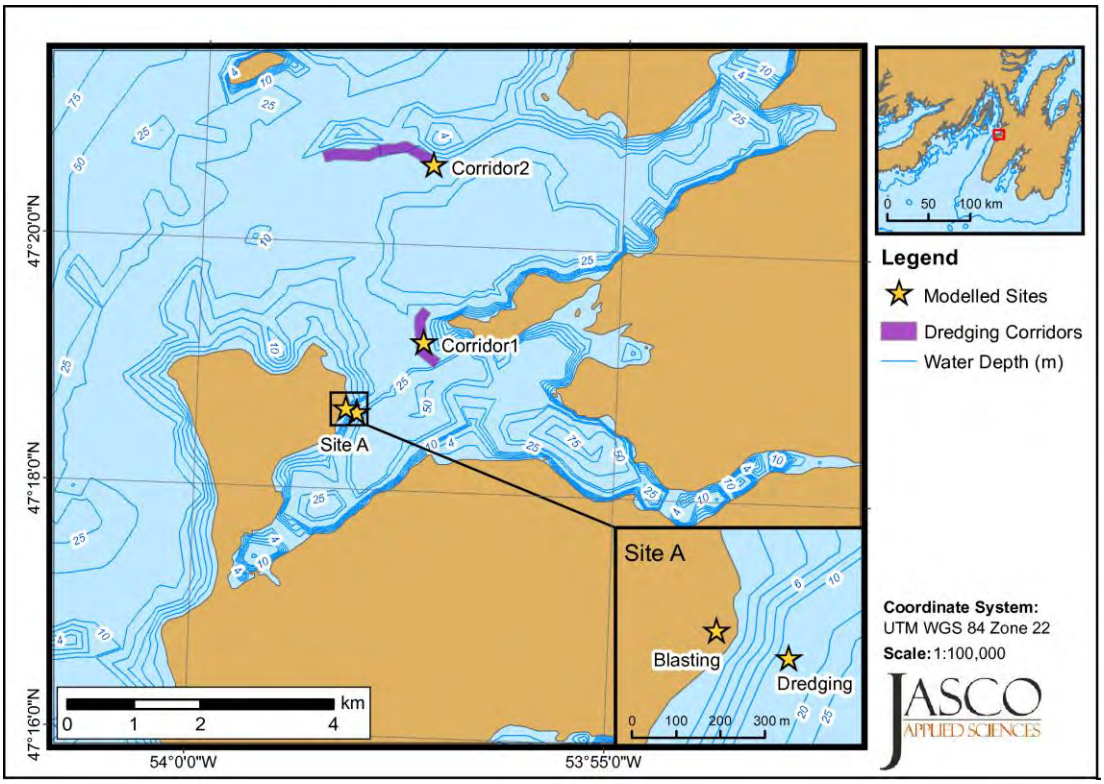

Figure 2-1 Overview of modelled sites near Argentia Harbour, Placentia Bay, NL, Canada

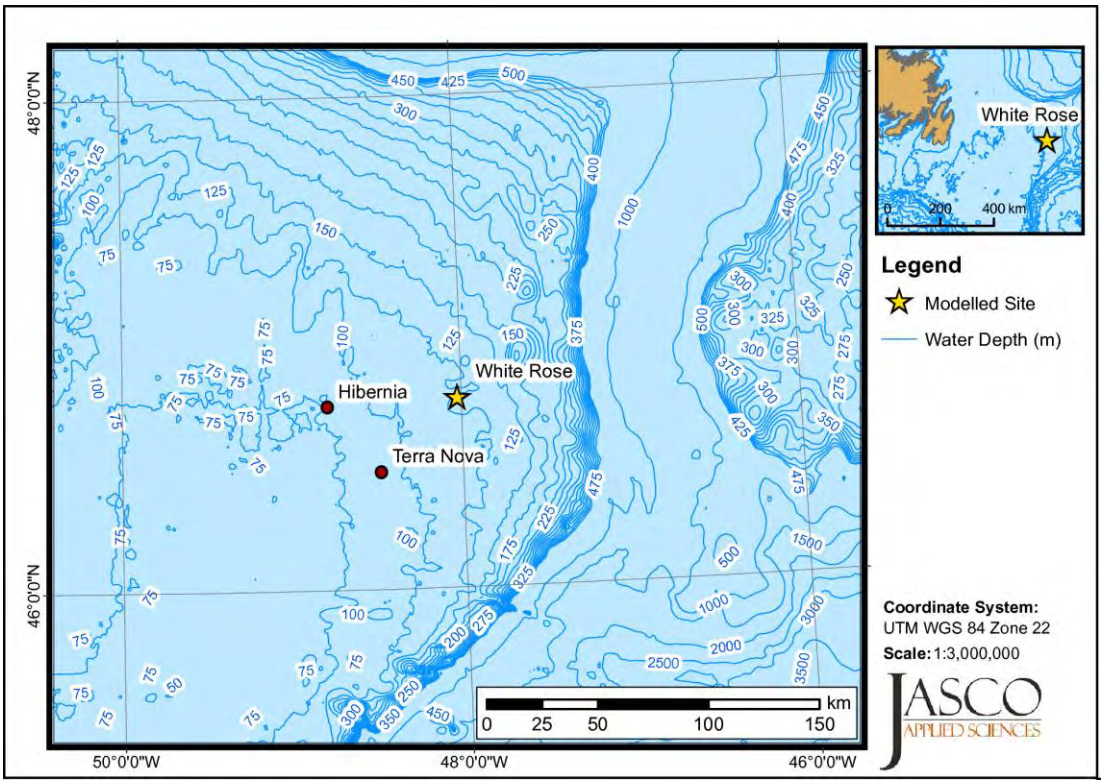

Figure 2-2 Overview of modelled site at the White Rose field, offshore Newfoundland, Canada

Table 2-1 Location and sound sources of each modelled scenario and the propagation model employed

Scenario	Location	Source	UTM Coordinates (m), Zone 22	Water depth (m)	Model
Nearshore					
1	Site A	1. Blasting (on-shore)	275500 E, 5244000 N	0	RAM-S
2	Site A	3. Dredging, cutter suction dredge	275663 E, 5243937 N	14.2	MONM
3	Corridor 1	2. Blasting (in water)	276672 E, 5244988 N	14.6	RAM-S
4	Corridor 1	4. Dredge, trailing suction hopper dredge	276672 E, 5244988 N	14.6	MONM
5	Corridor 2	4. Dredge, trailing suction hopper dredge	276825 E, 5247656 N	14.5	MONM
Offshore					
6	White Rose Field	4. Dredge, trailing suction hopper dredge	727202 E, 5184225 N	128.3	MONM
7	White Rose Field	5. Drilling	727202 E, 5184225 N	128.3	MONM
8	White Rose Field	6. Support vessel	727202 E, 5184225 N	128.3	MONM
9	White Rose Field	7. Helicopter	727202 E, 5184225 N	128.3	Young's equation

2.2 Acoustic Sources

The main sources of underwater acoustic noise from the WREP are expected to be generated during blasting, dredging and drilling . Lower acoustic levels are expected from the use of support vessels and helicopter. The source specifications relating to underwater acoustic modelling are summarized in Table 2-2. The method used to model the 1/3-octave band source levels are detailed in Sections 2.2.1 to 2.2.5.

Table 2-2 Acoustic source specifications

Source	Operation	Source Depth	BB SL (dB re 1 µPa @ 1 m)	Frequency range (kHz)	Propagation Model	Location
1	Blasting, on-shore	20 m below sea level	243.5	0.01–2	RAM-S	Site A
2	Blasting, off-shore	2 m below seafloor	243.5	0.01–2	RAM-S	Corridor 1
3	Dredging, cutter suction dredge	5 m, 1 m above seafloor (A)	189.3	0.01–10	MONM	Site A
4	Dredging, trailing suction hopper dredge	5 m, 1 m above seafloor (A)	195.4	0.01–10	MONM	Corridors 1 & 2, White Rose Field
5	Drilling	36 m	162.3	0.01–10	MONM	White Rose Field
6	Support vessel	5 m	182.5	0.01–10	MONM	White Rose Field
7	Helicopter	91 m above sea surface	169.7	0.01–10	N/A	White Rose Field

Note: The source depths are in metres (m)

(A) Dredging was modelled as two point sources, a low-frequency source close to the surface and the high-frequency source close to the seafloor (see details in Section 2.2.2

2.2.1 Sources 1 and 2: Blasting

Blasting operations may be performed to facilitate dredging if hard substrate is encountered. For this operation, explosive charges would be installed in pre-drilled holes at a few metres depth in the ground. At the time of modelling it was unknown if the blasting operation will be required; therefore, neither the contractor nor the specifics of the blasting operation were available. JASCO relied on previous experience modelling blasting (Matthews *et al.* 2010, Zykov *et al.* 2010) for selecting realistic parameters.

Blast overpressure levels at a receiver were modelled with the ConWep software. These levels were then back-propagated to estimate the source levels at a reference distance of 1 m. ConWep predicts ground-shock overpressures for specified charge sizes and detonation depths below the ground surface (Hyde 1988). It includes a database of the yield and detonation rates for various explosive compounds, including pentolite and trinitrotoluene (TNT). ConWep employs empirical equations developed on the basis of numerous experiments conducted by the US Army (TM 5-855-1 1986). For ground-shock modelling, ConWep predicts the peak pressure and peak pressure time-history curve (P-T history curve) envelope.

The input parameters for ConWep include the type and weight of the explosive charge, geometry of the blast (charge depth, distance and depth to the receiver) and geoacoustic parameters of the substrate (density, and P-wave speed and attenuation coefficient).

The P-T history curve was computed for a receiver located 40 m from the charge. Reflections from all other layers were excluded from modelling at this stage. The amplitude of the P-T curve was then back-propagated to 1 m assuming spherical spreading loss of $20\log_{10}(R/1\text{ m})$, where R is the distance at which the original P-T curve was estimated (i.e., 40 m).

The overpressure signature was modelled for a blast charge of 5 kg of pentolite, which is equivalent to 7.1 kg of TNT (Figure 2-3). The physical properties of the backfill sediments were set to simulate till (see Section 2.4.1): 2 000 m/s P-wave speed; and 2 000 kg/m^3 density. The acoustic wave excited by a blast is characterized by an instantaneous rise of pressure, followed by exponential decay. The frequency spectrum of such signal is more or less flat, i.e., the acoustic energy is distributed evenly among the frequency bands. The rms SPL and SEL metrics were calculated for the acoustic pulse at 1 m using Equations 1 and 2, respectively. The characteristics of the acoustic pulse from a 5 kg charge of pentolite are summarized in Table 2-3.

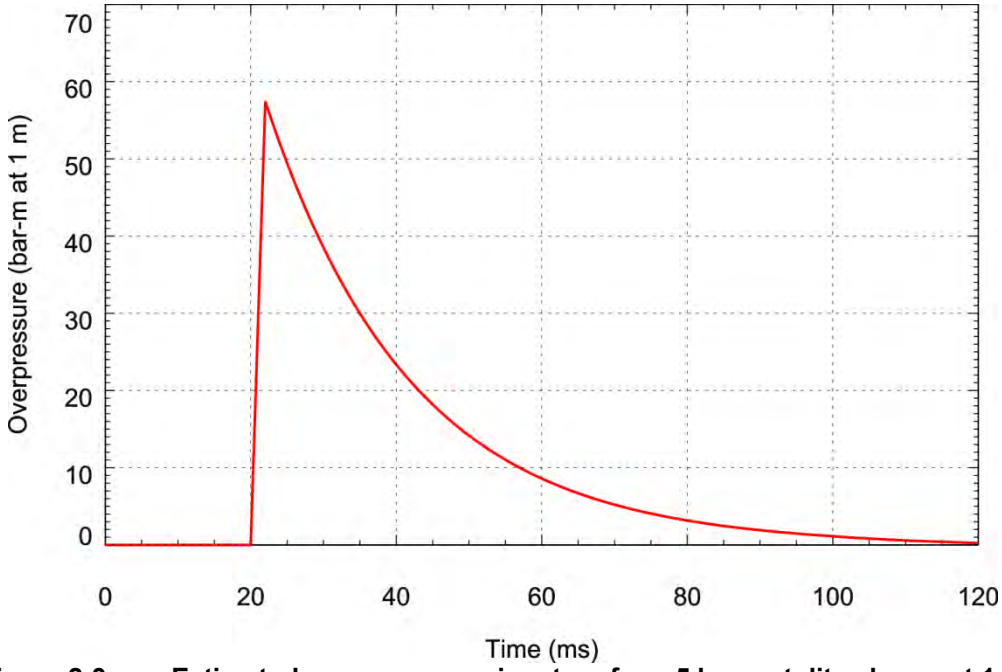

Figure 2-3 Estimated overpressure signature for a 5 kg pentolite charge at 1 m

Table 2-3 Estimated sound levels of the acoustic pulse produced by detonation of 5 kg of pentolite

Distance from source (m)	Zero-to-peak SPL (dB re 1 µPa)	rms SPL (dB re 1 µPa)	SEL (dB re 1 µPa^2·s)
40	219.1	211.4	199.3
1	255.1	243.5	231.5

The modelling of the acoustic wave propagation from the blast was performed in 24 1/3-octave bands (10 Hz to 2 kHz). The SEL in each band was calculated as 217.5 dB re 1 $\mu Pa^2 \cdot s$ by distributing the acoustic energy evenly through the bands.

2.2.2 Source 3 and 4: Suction Dredges

Suction dredges use a wide pipe (up to 1 m in diameter) and a high power pump to suck water and bottom material into a hopper or onto the shore. A cutter head may be used to help loosen sediment. The pipe with a cutter head or drag head can be steered using cables and winches or thrusters. Generally, a cutter suction dredge (CSD) vessel uses legs (also known as spuds) and swings between anchors instead of using a propulsion system. In contrast, a trailing suction hopper dredge (TSHD) vessel moves using its main propulsion system (propeller and/or thrusters).

During dredging operations, the main sources of underwater sound are the vessel's propulsion system and onboard machinery, the displacement of material by the suction head at the seafloor and the displacement of material through the suction pipe. Robinson et al. (2011) recorded six TSHD in several operational modes. His study shows that sound levels below 1 kHz are associated mainly with the vessel itself, while sound levels above 1 kHz are associated mainly with the dragging/abrasion of sediment passing through the drag head, suction pipe and pump. Beamforming analysis of recorded dredging noise from a number of TSHDs also shows that sound above a frequency of 2 kHz can be associated with the operations of the dredge pump and dredger head close to the seafloor (Robinson et al. 2011). Thus, suction dredges may be represented by a low-frequency source (< 1 to 2 kHz) close to the water surface and a higher-frequency source (> 2 kHz) close to the seafloor.

Various suction dredge spectra are presented in Figure 2-4; the known dredge specifications are summarized in Table 2-4. Generally, the source levels for TSHD, which uses the vessel's propulsion system, are higher than for CSD at < 1 kHz. This is in accordance with the Robinson et al. (2011) study.

While it is expected that a CSD will be used at Site A and a TSHD will be used for the dredging of Corridors 1 and 2, the exact specifications of the suction dredges to be used in the WREP are unknown. Thus, two source level spectra were constructed based on the source levels of the reference spectra in Figure 2-4. For each 1/3-octave band below 1 kHz, the source level for the CSD was set to the maximum level of all reference CSDs and the source level for the TSHD was set to the maximum level of all reference TSHDs. For each 1/3-octave band above 1 kHz, the source level for both the CSD and TSHD was set to the maximum level of all reference dredges (Figure 2-5).

In accordance with Robinson et al. (2011), the source depths of the suction dredges were set to 5 m depth for frequencies below 2 kHz and 1 m above the seafloor for frequencies above 2 kHz.

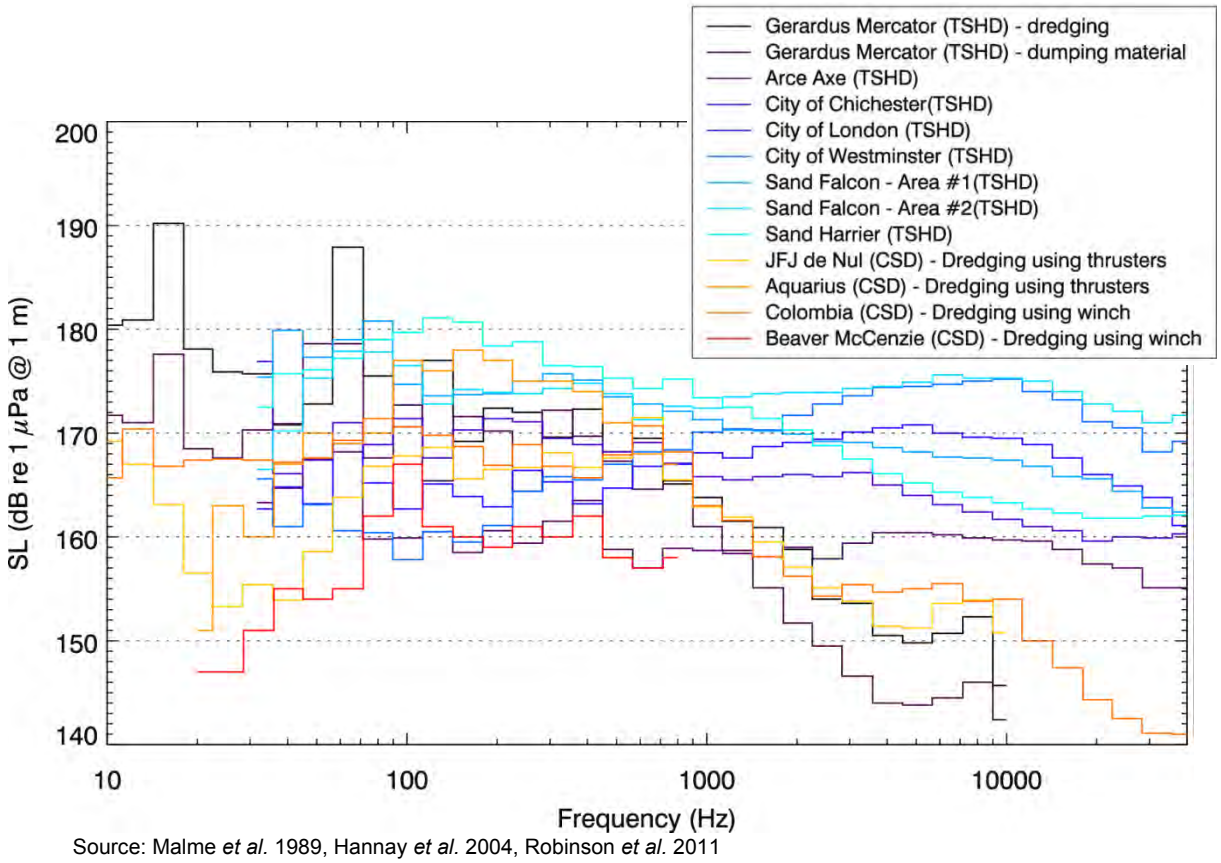

Source: Malme *et al.* 1989, Hannay *et al.* 2004, Robinson *et al.* 2011

Figure 2-4 Comparison of published source levels from trailing suction hopper dredges and cutter suction dredges

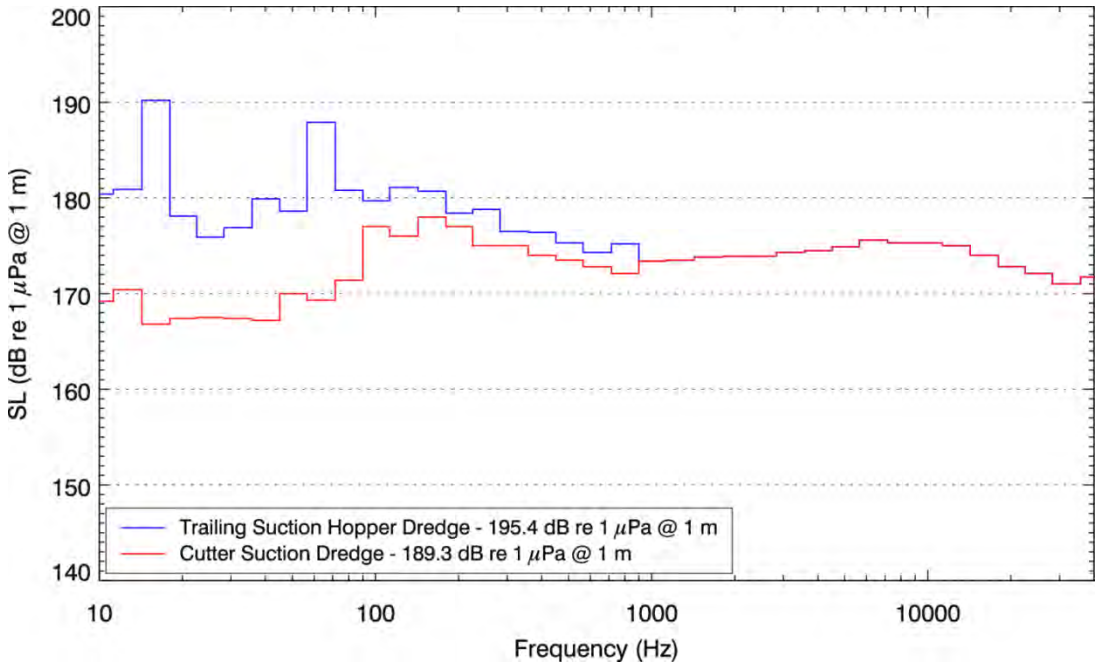

Figure 2-5 Estimated source levels for the modelled trailing suction hopper dredge and the cutter suction dredge

Table 2-4 Specifications of the reference dredges

Dredge	Type	Dimension (m)	Size/ tonnage	Max dredge depth (m)	Other specifications	Reference
Sand Harrier	TSHD	99	4671 t	33	Pump power: 1591 kW	Robinson et al. 2011
Sand Falcon	TSHD	120	8359 t	50	Pump power: 1100 and 1631 kW (2 pumps)	Robinson et al. 2011
Arco Axe	TSHD	98.3	5000 t	48	Pump power: 1100 kW	Robinson et al. 2011
City of Chichester	TSHD	72	2300 t	35	Pump power: 700 kW	Robinson et al. 2011
City of London	TSHD	99.9	4750 t	46	Pump power: 1100 kW	Robinson et al. 2011
City of Westminster	TSHD	99.7	5200 t	46	Pump power: 1100 kW	Robinson et al. 2011
Gerardus Mercator	TSHD	152.9 × 29 × 11.51	hopper size: 18 000 m³	112	Suction pumps, double-walled 2 × 3000 kW Discharge pumps power 14 000 kW Submerged dredgepump 3200 kW Main engines 2 × 9450 kW Shaft generators 2 × 4500 kW Auxiliary engines 3 × 924 kW Harbour engine 320 kW Jet pumps 2 × 1000 kW Bow thrusters 2 × 1000 kW	Hannay et al. 2004 http://www.sakhalinenergy.com/en/documents/doc_33_cea_tbl4-7.pdf
JFJ de Nul	CSD	124.4 × 27.8 × 6.51	unknown	35	Cutter head controlled by thruster Cutter drive power 6000 kW Submerged dredge pump on cutter ladder 3 800 kW Inboard dredge pumps 2 × 6000 kW Propulsion 2 × 3800 kW Total installed power 27 190 kW	Hannay et al. 2004 http://www.sakhalinenergy.com/en/documents/doc_33_cea_tbl4-7.pdf
Aquarius	CSD	107 × 19 × 4.85	unknown	25	12 889 kW Cutter head controlled by thruster	Malme et al. 1989
Columbia	CSD	49 × 13.4 × 2.14	unknown	18	Pipe diameter: 0.66 m Cutter power: 375 kW Total power: 3954 kW Cutter head controlled by winch	Zykov et al. 2007

Dredge	Type	Dimension (m)	Size/ tonnage	Max dredge depth (m)	Other specifications	Reference
Beaver MacKenzie	CSD	86.5 × 15.44 × 4	2148.5 t	45	Pipe Diameter: 0.85 m 1500 hp on ladder; 1700 hp on discharge; 1500 hp on jet pump Cutter head controlled by winch	Malme et al. 1989

2.2.3 Source 5: Drilling Platform

The planned WHP consists of a CGS with a topside that includes drilling facilities, wellheads and support services (i.e., accommodations, utilities, flare boom and helideck) (Figure 2-6). Although underwater sound levels from multiple types of drilling installations (e.g., drillships, semi-submerged platforms, fixed multi-legged platforms and drilling islands) are publicly available, recordings of drilling operations from a WHP are limited (Gales 1982, Malme *et al.* 1989, Richardson *et al.* 1995, Blackwell *et al.* 2004, Hannay *et al.* 2004). In general, drillships produce higher sound levels than fixed multi-legged platforms (Gales 1982), whereas drilling islands produce the lowest sound levels (Blackwell et al. 2004).

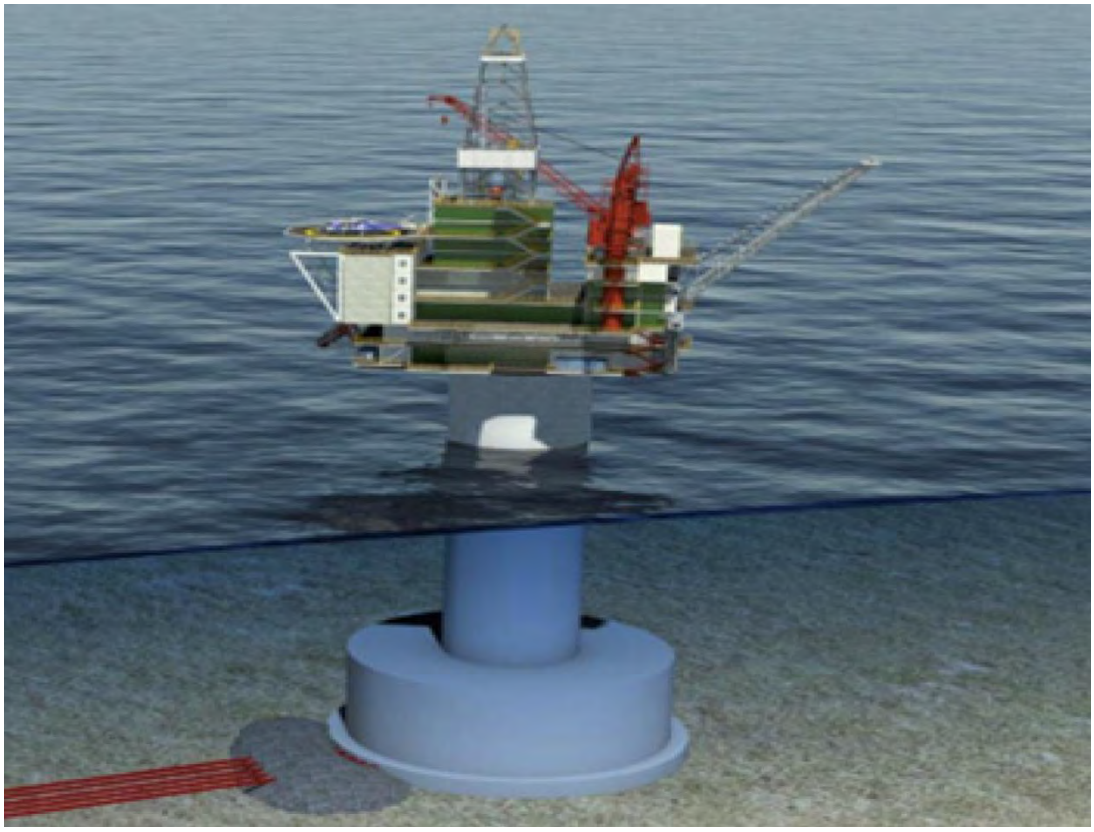

Source: Husky Energy 2012

Figure 2-6 Example of a wellhead platform with a concrete gravity structure

In this study, source levels for the drilling operations at the WHP were estimated from JASCO recordings of the *Molikpaq* platform while drilling (Hannay et al. 2004). The *Molikpaq* drilling platform is a 111 m wide, caisson-retained platform (i.e., ballast is filled with sand), located 16 km offshore northeast Sakhalin, Russia. Received levels from these recordings were back-propagated assuming spherical spreading loss, to conservatively estimate the source levels (Figure 2-7).

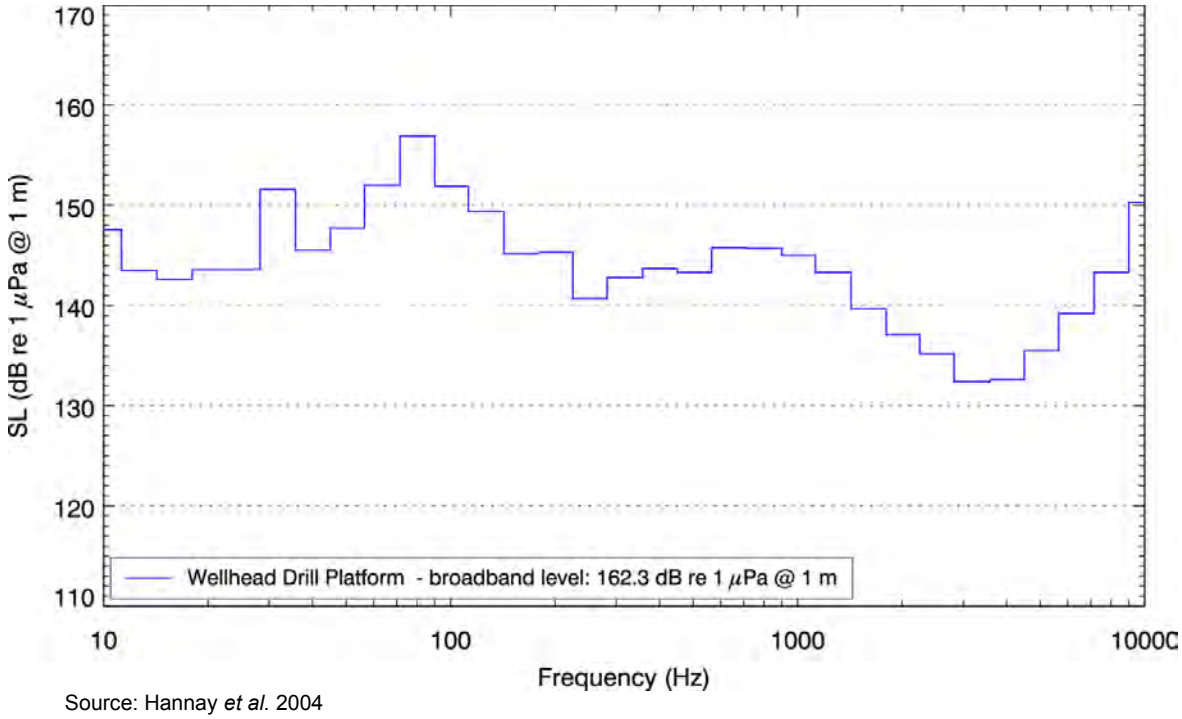

Source: Hannay *et al.* 2004

Figure 2-7 Estimated 1/3-octave band source levels for drilling operations at the modelled wellhead platform, based on source levels for the caisson-retained *Molikpaq* platform

Sound may come from multiple locations on the platform, including the machinery outside the water, resonances along the caisson and the drill within the seafloor. The depth of the source influences sound propagation by creating a cut-off frequency in the spectrum. This cut-off frequency can be seen as a low-frequency (or high-pass) filter; sound propagating at frequencies below the cut-off value is highly attenuated since the source depth is less than one-quarter of the frequency wavelength. To produce a cautionary estimate of distances to sound level thresholds, sound from the drilling operations was modelled as a point source located at 36 m depth, equal to one-quarter of the wavelength of the lowest modelled frequency, which is 144 m at 10 Hz. This source depth minimizes the attenuation of low frequencies and promotes long-range propagation.

2.2.4 Source 6: Support Vessel

Tugs often work at high-power output rates. As such, the cavitation process of the propeller blades and/or the use of jet thrusters are the main sources of underwater sound. The intensity of these sources is generally related to the vessel's total horsepower (Hannay et al. 2004).

At the time of this study, the support vessel at the White Rose field was expected to be a tug with a power of approximately 5 000 HP. Since the exact vessel was undetermined, a reference vessel recorded by JASCO, the *Neftegaz 22* (Hannay et al. 2004), was chosen to represent the support vessel based on its total horsepower. The *Neftegaz 22* specifications are:

- Type: anchor handling tug supply

- Built: 1985, Poland
- Deadweight: 1 397 metric tonnes
- Length overall: 81 m
- Breath: 16 m
- Draft: 4.9 m (loaded light)
- Engines: 2×6 ZL 40/48
- Total break-horsepower (BHP): 7 200
- Maximum speed: 26 km/h (14 knots)

The 1/3-octave band source levels of the modelled support vessel were adjusted for the difference in total horsepower (THP) between the two vessels (-1.5 dB) using the following equation:

$$SL = SL_{ref} + 10\log\left(\frac{THP}{THP_{ref}}\right) = SL_{ref} + 10\log\left(\frac{5000\ HP}{7200\ HP}\right) \quad (4)$$

The final spectrum for the modelled support vessel is presented in Figure 2-8.

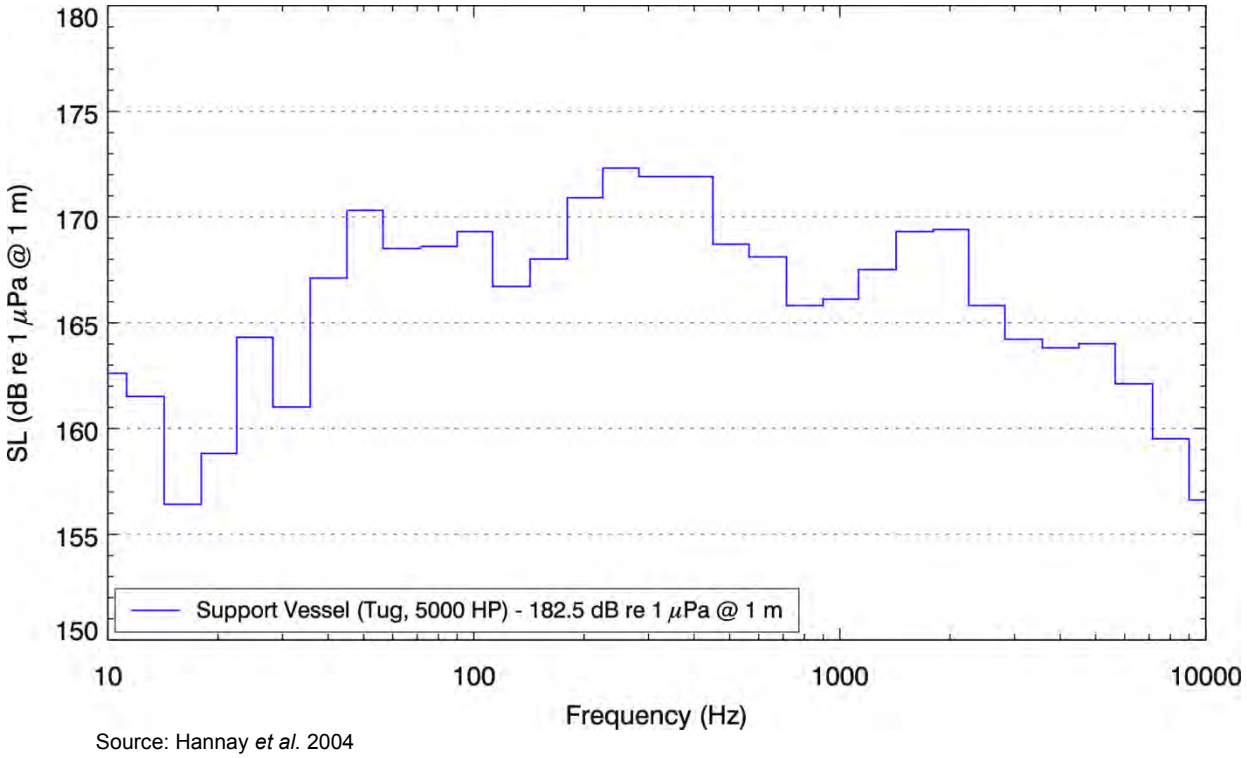

Source: Hannay *et al.* 2004

Figure 2-8 Estimated source levels for the support vessel based on the surrogate tug, *Neftegaz 22*

Since the propulsion system and the onboard machinery (propagating through the hull) is generally the sound source in tug operations, the depth of the modelled source was set to 5 m, a conservatively large estimate of the vessel draft.

The depth of the source influences sound propagation by creating a cut-off frequency in the spectrum. This cut-off frequency can be seen as a low-frequency (or high-pass) filter; sound propagating at frequencies below the cut-off value is highly attenuated since the source depth is less than one-quarter of the frequency wavelength. The cut-off frequency for a source depth of 5 m is approximately 73 Hz (based on the average underwater sound speed at the White Rose site). Since lower frequencies generally propagate further from a source, a similar vessel with a shallower draft (e.g., 3.5 m, leading to a cut-off frequency of approximately 103 Hz) would result in shorter distances to sound level thresholds.

2.2.5 Source 7: Helicopter

At the time of this study, the type of helicopter to be used for the WREP was unknown. JASCO recordings of a Bell 206 and a Bell 212 helicopter were used to estimate source levels. These helicopters were recorded during low-speed fly pass, and spectrum levels were backpropagated to the reference distance of 1 m, assuming spherical spreading loss of $20\log_{10}(R/1\text{ m})$, where R is the distance between the receiver and the helicopter. The helicopter specifications and 1/3-ocatve band spectrum are presented in Table 2-5 and Figure 2-9. Note that the standard reference pressure for underwater acoustics (1 µPa) differs from in-air acoustics (20 µPa). However, the source levels for the recorded helicopters are presented in reference to 1 µPa for comparison purposes. For cautionary results, the assessment of underwater received levels from the helicopter was modelled using the highest source levels (i.e., the Bell 206 helicopter).

Table 2-5 Specifications of reference helicopters

Type	Specifications/Comments
Bell 206	• Length: 12.11 m • Rotor diameter: 10.16 m • Height: 2.83 m • Disc area: 81.1 m² • Powerplant: 1 × Allison 250-C20J turboshaft, 420 shp (310 kW) • Maximum speed: 130 knots (224 km/h)
Bell 212	• Length: 17.43 m • Rotor diameter: 14.64 m • Height: 3.83 m • Disc area: 168.3 m² • Powerplant: 1 × Pratt & Whitney Canada PT6T-3 or −3B turboshaft, 1800 shp (1342 kW) • Maximum speed: 120 knots (223 km/h)

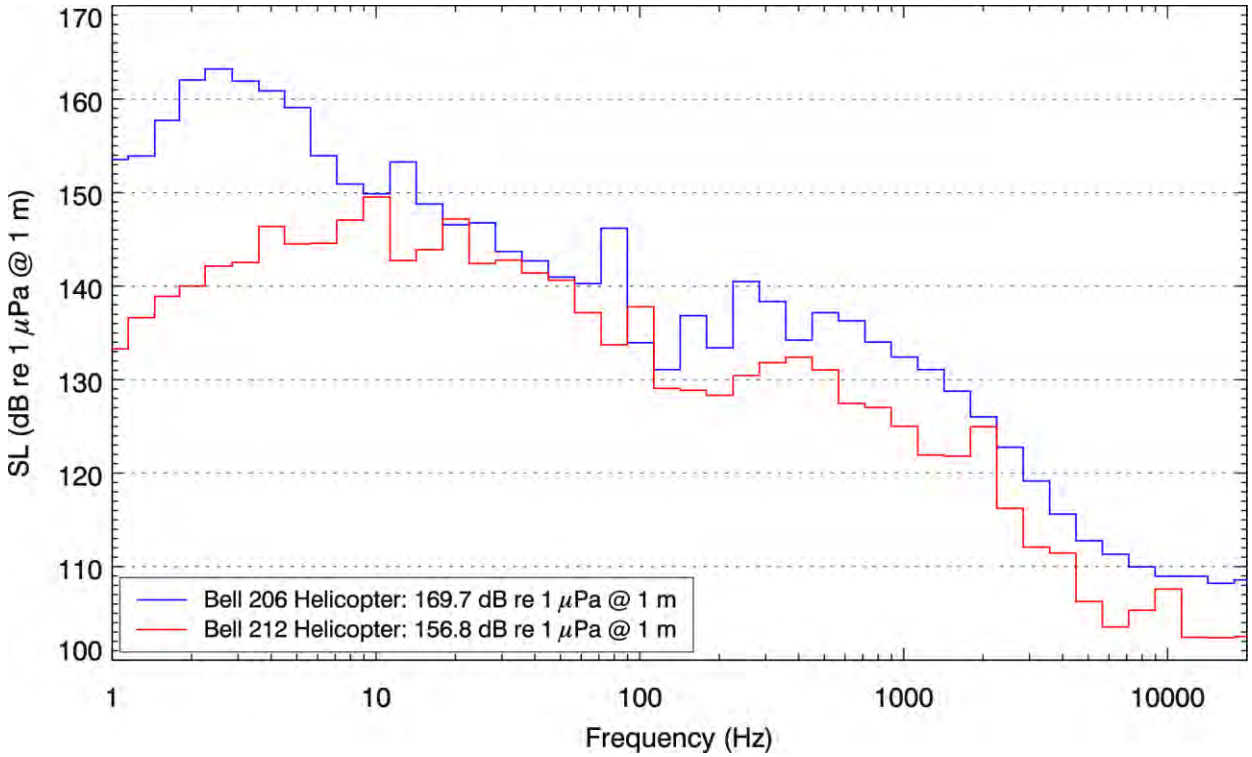

Figure 2-9 Calculated 1/3-octave band source levels for Bell 206 and Bell 212 helicopter

2.3 Sound Propagation Models

Sound was propagated through the underwater environment using one or multiple propagation models. The selection of an appropriate propagation model was mainly based on the source's location (in-ground, in-water or in-air) and its frequency spectrum.

2.3.1 Source 1 and 2: Blasting

Blasting operations are performed by detonating explosive charges placed in the ocean-floor sediments. For modelling purposes, an explosion is considered to be an in-ground point source.

Marine sediment is an elastic medium that, unlike water, supports the propagation of shear waves. Simplified acoustic wave propagation models (e.g., Range-dependent Acoustic Model (RAM)) do not account for the existence of shear waves in the sediments. Shear waves are excluded from the models for a speedier modelling process. Exclusion of shear waves from the modelling is justifiable for an in-water source, and the observed reduction in the accuracy of the solution is acceptable. However, propagation modelling of an in-ground source without considering the presence of shear waves in the sediments can lead to an unacceptable loss of accuracy.

2.3.1.1 Range-dependent Acoustic Model with Shear Waves

Sound propagating from an explosive charge was modelled with RAM-S (Collins 1993). RAM-S is an extension of RAM that incorporates the propagation of shear waves in the sediments.

RAM-S incorporates five geoacoustic properties of the sediment layer: P-wave speed and attenuation, S-wave speed and attenuation, as well as sediment density. All five properties, as well as water depth and sound speed profiles in the water column, can be defined as a range-dependent vertical profile (i.e., each parameter varies with depth and distance from the source). RAM-S computes acoustic fields in three dimensions by modelling transmission loss along 2-D vertical radial planes covering a 360° swath from the source, an approach commonly referred to as N×2-D. RAM-S model results have been validated against controlled acoustic propagation experiments in a laboratory (Collis et al. 2007).

2.3.1.2 Model Parameters

In this study, sound transmission loss was modelled at the centre frequencies of 1/3-octave bands between 10 Hz and 2 kHz, for a total of 24 bands. This frequency range includes the important bandwidths of noise emissions for the blasting operation. The 2-D radial planes were evenly spaced covering a 360° swath with a separation angle of 2.5°, for a total of N=144 radials. The range step size along each radial was variable depending on the modelled frequency. For the frequency range from 10 to 63 Hz, the step size was 5 m; for the 80 Hz to 250 Hz range, 2 m; and for the 320 Hz to 2 kHz range, 1 m. Sound was modelled to a maximum range of 75 km at both Site A and Corridor 1.

2.3.1.3 Estimating 90 Percent Root-mean-square Sound Pressure Level from Sound Exposure Levels

Existing safety radius regulations for impulsive sound sources are based on the rms SPL metric. An objective definition of pulse duration is needed when measuring the rms level for a pulse. Following suggestions by Malme et al. (1986), Greene (1997) and McCauley et al. (1998), pulse duration is conventionally taken to be the interval during which 90 percent of the pulse energy is received. Although one can measure the 90 percent rms SPL in situ, this metric is generally difficult to model because the adaptive integration period, implicit in the definition of the 90 percent rms SPL, is sensitive to the specific multipath arrival pattern from the source and can vary greatly with distance from the source or with depth of the receiver. To predict the 90 percent rms SPL, it is necessary to model the full waveform of acoustic pressure, but full-waveform modelling for large-depth, range-dependent environments can be prohibitive due to the extensive time required to run the model.

In various studies where the rms SPL, SEL and pulse duration have been measured for individual airgun pulses, the offset between rms SPL and SEL is typically 5 to 15 dB, with considerable variation depending on water depth and geoacoustic environment (Greene 1997, McCauley *et al.* 1998, Blackwell *et al.* 2007, MacGillivray *et al.* 2007). Generally, the measured SEL to rms SPL offsets are larger at closer distances, where the pulse duration is short ($\ll$ 1 s), and smaller at farther distances, where the pulse duration tends to increase because of propagation effects.

In this study, JASCO's full-waveform acoustic propagation model FWRAM was used to determine range-dependent estimates of rms SPL and SEL for a small set of representative propagation directions.

FWRAM conducts time-domain calculations and is therefore appropriate for computing time-averaged rms SPLs for impulsive sources. The model computes synthetic pressure waveforms versus range and depth for range-varying marine acoustic environments using the parabolic equation (PE) approach to solving the acoustic wave equation. Like RAM-S, FWRAM accounts for range-varying properties of the acoustic environment. It uses the same environmental inputs (bathymetry, water sound speed profile and seabed geoacoustic profile). However, FWRAM computes pressure waveforms via Fourier synthesis[1] of the modelled acoustic transfer function in closely spaced frequency bands.

Range-dependent rms SPL-SEL conversion functions were calculated from the resulting rms SPL-SEL offsets and applied to the set of SEL predictions from RAM-S. This approach combines accurate pulse length information available from FWRAM with the greater computational efficiency of RAM-S.

The chosen propagation directions were along the azimuth where sound propagates farthest from the source (without traveling to land) (i.e., 015° east of UTM north at Site A and 310° at Corridor 1). The site-specific offset functions used in this study are presented in Figures 2-10 and 2-11.

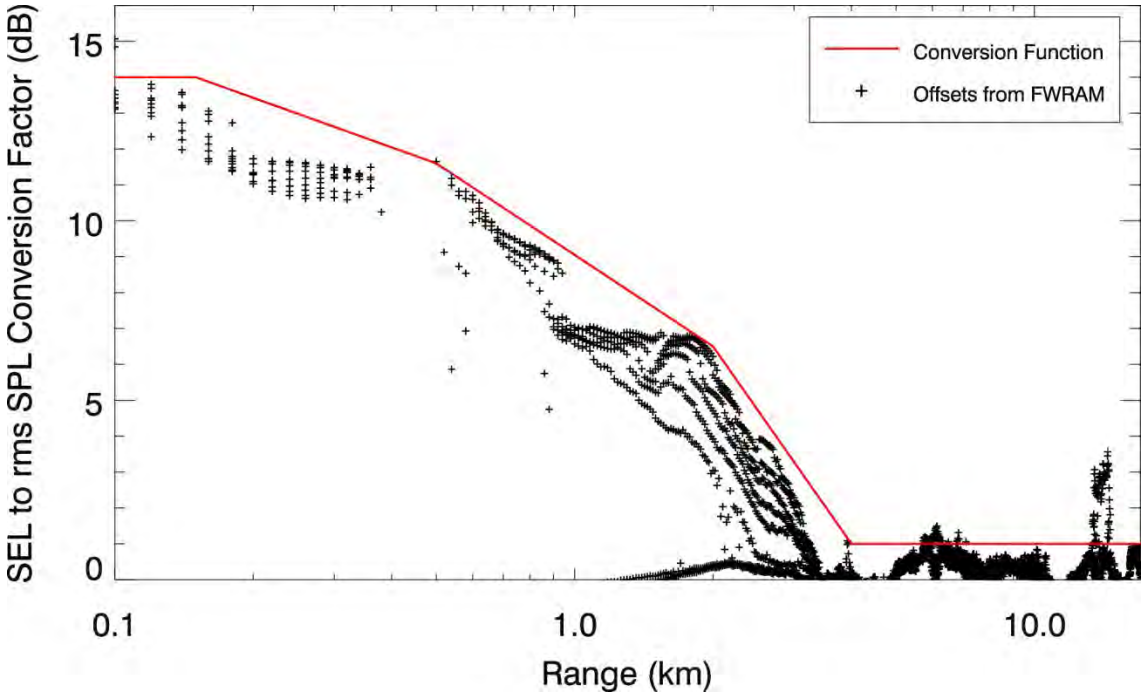

Figure 2-10 Offset of SELs to rms SPLs modelled for Site A

[1] Fourier synthesis is the operation of rebuilding a function from simpler pieces (Fourier series).

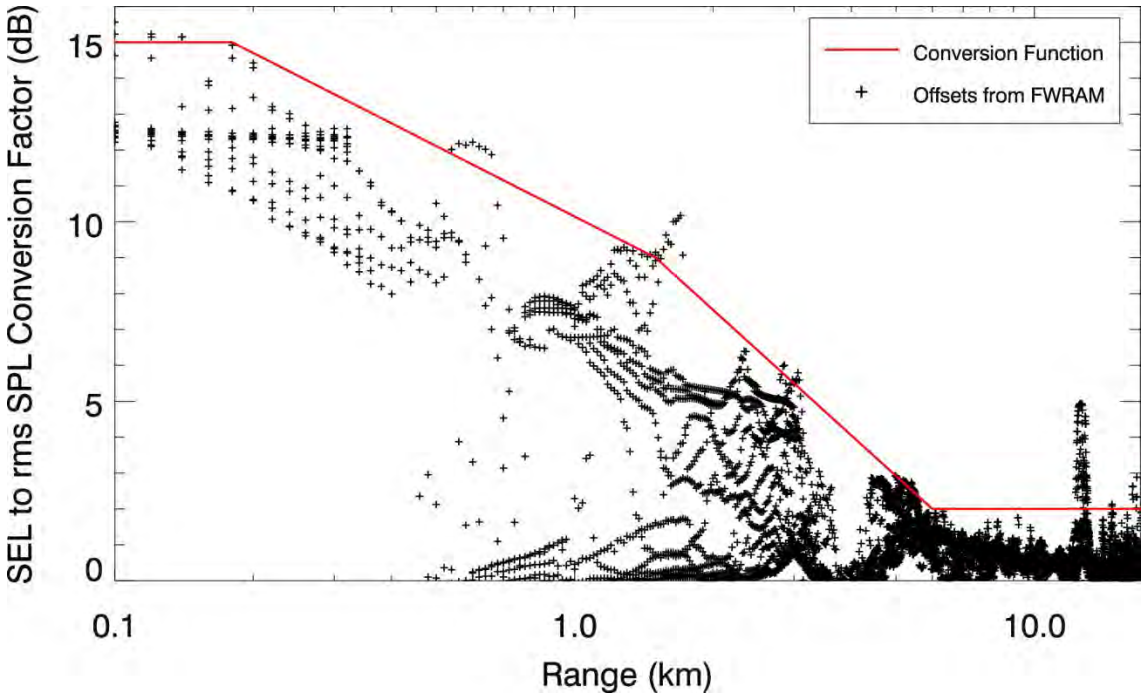

Figure 2-11 Offset of SELs to rms SPLs modelled for Corridor 1

2.3.2 Sources 3 to 6: Dredging, Drilling and Support Vessel

The acoustic propagation model used to model the acoustic sources at frequencies below 10 kHz is JASCO's Marine Operations Noise Model (MONM). MONM computes received SEL for impulsive sources. For a continuous source, such as a vessel, dredge or drill rig, MONM outputs rms SPLs.

MONM computes acoustic fields in three dimensions by modelling transmission loss along 2-D vertical radial planes covering a 360° swath from the source (*N*×2-D). MONM fully accounts for depth and/or range dependence of several environmental parameters, including bathymetry and the sound speed profiles in the water column and the sub-bottom. It also accounts for the additional reflection loss due to partial conversion of incident compressional waves to shear waves at the seabed and sub-bottom interfaces. It includes wave attenuations in all layers. The acoustic environment is sampled at a fixed range step within the radial planes.

MONM handles frequency dependence by computing acoustic transmission loss at the centre frequencies of 1/3-octave bands. It treats sound propagation through a wide-angled PE solution at frequencies ≤ 2 kHz and through a ray-tracing solution at frequencies > 2 kHz. Third-octave band received levels are computed by subtracting band transmission loss values from the corresponding directional source levels. Broadband received levels are then computed by summing the received band levels.

MONM's sound level predictions have been extensively validated against experimental data (Hannay and Racca 2005, Aerts *et al.* 2008, Funk *et al.* 2008, Ireland *et al.* 2009, O'Neill *et al.* 2010, Warner *et al.* 2010). An inherent variability in measured sound levels is caused by temporal variability in the environment (and the variability in the signature

of repeated acoustic impulses for non-continuous sources); sample sound source verification results are presented in Figure 2-12. While MONM's predictions correspond to the averaged received levels, cautionary estimates of the threshold radii are obtained by shifting the best fit line (solid line, Figure 2-12) upward so that the trend line encompasses 90 percent of all the data (dashed line, Figure 2-12).

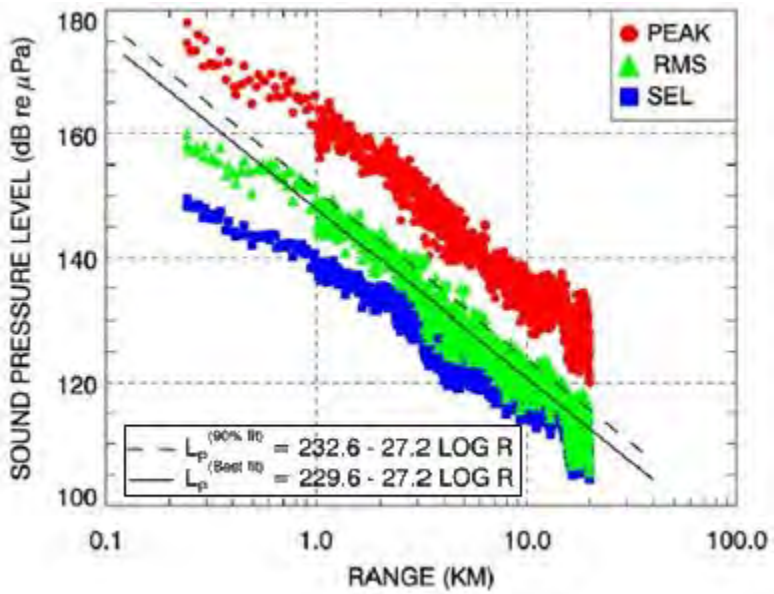

Source: Ireland *et al.* 2009

Solid line is the least squares best fit to rms SPL. Dashed line is the best fit line increased by 3.0 dB to exceed 90 percent of all rms SPL values (90th percentile fit)

Figure 2-12 Peak and rms SPL and per-shot SEL versus range from a 20 in^3 airgun array

In the regions of the Beaufort and Chukchi Seas, sound source verification results show that this 90th percentile best-fit is, on average, 3 dB higher than the original best fit line for sources in water depths greater than 20 m (Aerts *et al.* 2008, Funk *et al.* 2008, Ireland *et al.* 2009, O'Neill *et al.* 2010). Consequently, a safety factor of 3 dB was added to the predicted received levels to provide cautionary results reflecting the inherent variability of sound levels in the modelled area.

2.3.2.1 Marine Operations Noise Model: Range-dependent Acoustic Model

At frequencies up to 2 kHz, MONM treats sound propagation in range-varying acoustic environments through a wide-angled PE solution to the acoustic wave equation. The PE method used by MONM is based on a version of the Naval Research Laboratory's RAM, which has been modified to account for an elastic seabed. The PE method has been extensively benchmarked and is widely employed in the underwater acoustics community (Collins 1993).

2.3.2.2 Marine Operations Noise Model: BELLHOP

At frequencies between 2 and 10 kHz, MONM treats sound propagation in range-varying acoustic environments through ray-series approximation of the acoustic wave equation using the BELLHOP acoustic ray-trace model (Porter and Liu 1994).

BELLHOP models transmission loss in the ocean using the Gaussian beam tracing technique. In addition to other types of attenuation, BELLHOP accounts for sound attenuation due to energy absorption through ion relaxation and viscosity of water (Fisher and Simmons 1977). This type of attenuation is important for frequencies higher than 5 kHz and cannot be neglected without noticeable effect on the modelling results at longer distances from the source (may be > 3 dB at approximately 10 km from the source for frequencies ≥ 5 kHz).

2.3.2.3 Model Parameters

In this study, sound transmission loss was modelled at the centre frequencies of 1/3-octave bands between 10 Hz and 10 kHz. This frequency range includes the important bandwidths of noise emissions for the modelled dredging, drilling and support vessel operations. The 2-D radial planes were evenly spaced covering a 360° swath with a separation angle of 2.5°, for a total of N=144 radials. At all frequencies the range step size along each radial was 5 m. Sound was modelled to a range of 25 km at Sites A, Corridor 1 and Corridor 2, and 50 km at the White Rose field site.

2.3.3 Source 7: Helicopter

The large difference in acoustic impedance between air and water limits the amount of sound energy that can penetrate the sea surface and propagate underwater. According to Snell's law, sound propagating at angles > 13° from vertical will be totally reflected at the sea surface ((5) in Figure 2-13). Some sound energy may penetrate the water at angles > 13° in conditions of high sea state (Lubard and Hurdle 1976), or via scattering ((4) in Figure 2-13); however, most of the received energy far from the source is transmitted through direct- and bottom-reflected paths ((1) to (3) in Figure 2-13).

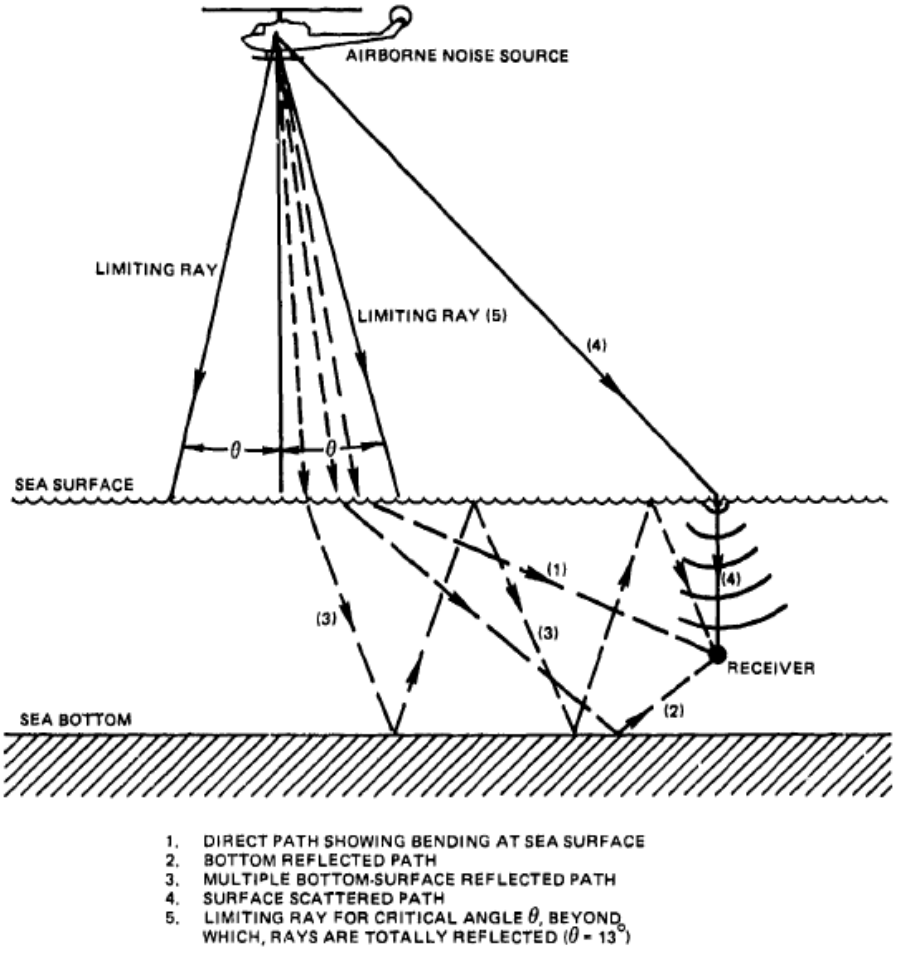

Source: Gales 1982, based on Urick 1972

Figure 2-13 Ray-path diagram for air-water propagation from an airborne source

Received underwater sound levels strongly depend on the altitude of the aircraft and the water depth. Received levels tend to be higher in shallow environments with a reflective bottom; however, reported underwater received levels for helicopters are low (Urick 1972, Young 1973, Greene 1985, Richardson and Malme 1993, Richardson *et al.* 1995). For example, Greene (1985) reports:

- Recorded levels of no higher than 111 dB re 1 µPa at 9 m below the surface, directly under a Bell 212 helicopter flying at an altitude of 305 m

- Recorded levels no higher than 111 dB re 1 µPa at 9 m below the surface, at a lateral distance of 50 m from a Sikorsky 61 helicopter flying at an altitude of 152 m.

Richardson (1995) also presents relatively low levels for three types of helicopters flying at an altitude of 300 m (see Figure 2-14).

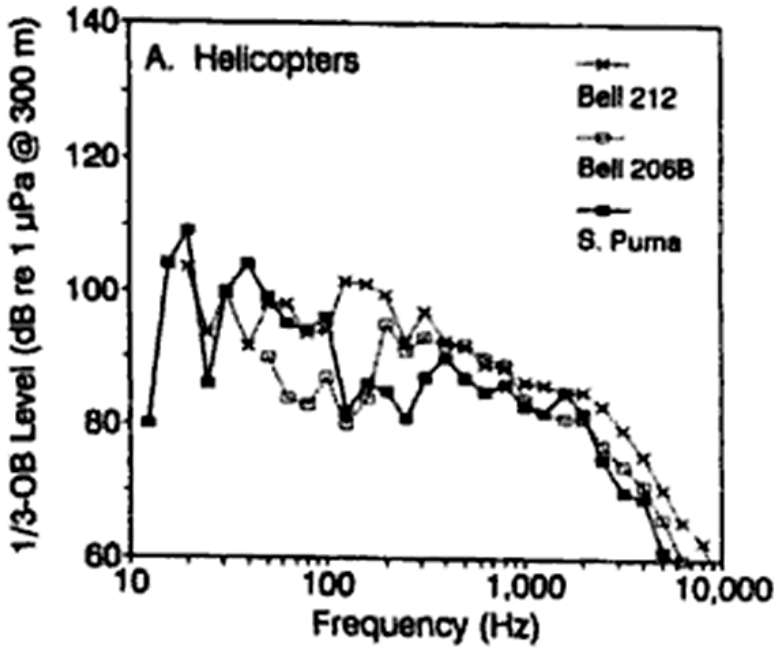

Source: Richardson *et al.* 1995, Figure 6.4

Figure 2-14 Derived 1/3-octave band levels at the water surface, directly below helicopters flying at an altitude of 300 m

2.3.3.1 Young's Model

Underwater received levels from an airborne source may be estimated using Young's equation (1973), which produces results consistent with empirical data (Richardson et al. 1995). Young's equation estimates underwater acoustic (broadband) levels from an airborne source though the computation of a virtual source. This virtual source accounts for the changes in sound speed and path angles due to changes in impedance between air and water.

2.3.3.2 Model Parameters

In this report, distances to the 120 dB re 1 µPa (rms SPL) threshold were estimated using Young's tabulated transmission loss levels for an airborne source at 91 m (300 ft), corrected for expected averaged sound speed in water at the White Rose field (1 441 m/s in February, 1 471 m/s in August). Distances to other level thresholds (i.e., ≥ 130 dB re 1 µPa) were estimated assuming spherical spreading. This is a valid assumption since the distances to the 120 dB re 1 µPa are estimated to be less than half the water depth.

2.4 Environmental Parameters

2.4.1 Nearshore: Site A, Corridors 1 and 2

Water depths throughout the Argentia Harbour and Placentia Bay areas were obtained from soundings and bathymetric contour data from navigational charts (Canadian Hydrographic Services 2012). The data sets were merged and re-gridded, using bilinear

interpolation, onto a Universal Transverse Mercator (UTM) Zone 22 coordinate projection with a horizontal resolution of 25 × 25 m.

The bottom geology and the geoacoustic properties within Argentia Harbour and Placentia Bay were obtained from reports by C-CORE provided by Stantec (Halliday 2012, Halliday and Cuff 2012) and from published literature (Catto et al. 1997). Generally, the surficial sediments in the area include layers of medium to fine-grained sand and gravel, underlain by till or bedrock. The thickness of surficial layers increases to the southwest, from outcrops of till in the north to 8 m of sand west of Site A.

The geoacoustic properties were estimated following equations by Hamilton (1980) and Buckingham (2005). Three geoacoustic profiles were developed to represent the geoacoustic conditions for:

- Onshore blasting operations near Site A (Table 2-6)
- The fine-grained sand found at and around Site A (Table 2-7)
- The medium-grained sand found at and around Corridors 1 and 2 (Table 2-8).

The geoacoustic profile for modelling of blasting operations has no top layer of soft sediments (sand or gravel), since the blasting operation will be performed once highly-compacted sediments are encountered (till or bedrock) and the blast charges will be placed in sediment that is difficult to remove with the dredge alone.

Table 2-6 Geoacoustic profile for onshore blasting operation near Site A

Sediment	Depth (m)	Density (g/cm^3)	Compressional sound speed (m/s)	Compressional sound attenuation (dB/λ)	Shear sound speed (m/s)	Shear sound attenuation (dB/λ)
Till	0 to 40	2.1 to 2.3	2000 to 2500	1.0	400	0.4
	40 to 100	2.3 to 2.6	2500 to 3000	1.0 to 0.3	400	0.4
	100 to 255	2.6 to 2.6	3000	0.3	400	0.4
Precambrian Bedrock	> 255	2.60	5500	0.28	400	0.4

Table 2-7 Geoacoustic profile for Site A

Sediment	Depth (m)	Density (g/cm^3)	Compressional sound speed (m/s)	Compressional sound attenuation (dB/λ)	Shear sound speed (m/s)	Shear sound attenuation (dB/λ)
Sand and Gravel	0 to 1	2.0	1606 to 1723	0.30 to 0.40	200	2.0
	1 to 6	2.04-2.10	1723 to 2000	0.40 to 1.00		
Till	6 to 255	2.10-2.60	2000 to 5500	1.00 to 0.28		
Precambrian Bedrock	> 255	2.60	5500	0.28		

Table 2-8 Geoacoustic profile for Corridors 1 and 2

Sediment	Depth (m)	Density (g/cm^3)	Compressional sound speed (m/s)	Compressional sound attenuation (dB/λ)	Shear sound speed (m/s)	Shear sound attenuation (dB/λ)
Sand and Gravel	0 to 1	2.0	1650 to 1805	0.60	250	3.0
	1 to 6	2.08-2.10	1805 to 2000	0.60 to 1.00		
Till	6 to 255	2.10-2.60	2000 to 5500	1.00 to 0.28		
Precambrian Bedrock	> 255	2.60	5500	0.28		

Underwater sound speed profiles for Argentia Harbour and Placentia Bay were downloaded from the US Naval Oceanographic Office's Generalized Digital Environmental Model (GDEM) database (Teague et al. 1990). The latest release of the GDEM database (version 3.0) provides average monthly profiles of temperature and salinity for the world's oceans on a latitude/longitude grid with 0.25° resolution. GDEM profiles are provided at 78 fixed depths to a maximum depth of 6800 m. They are based on historical observations of global temperature and salinity from the US Navy Master Oceanographic Observational Data Set (MOODS).

Temperature-salinity profiles were extracted from the GDEM database for the appropriate season and source location and were converted to speed of sound in seawater (*c*, m/s) using the equations of Coppens (1981):

$$\begin{aligned} c(z,T,S) &= 1449.05 + 45.7t - 5.21t^2 - 0.23t^3 \\ &\quad + (1.333 - 0.126t + 0.009t^2)(S-35) + \Delta \\ \Delta &= 16.3Z + 0.18Z^2 \\ Z &= (z/1000)(1 - 0.0026\cos(2\phi)) \\ t &= T/10 \end{aligned} \quad (5)$$

where *z* is water depth (m), *T* is temperature (°C), *S* is salinity (psu) and Φ (Phi) is latitude (radians). The resulting monthly sound speed profiles are shown in Figure 2-15. The sound fields were modelled using two profiles: that with the most constant sound speed (February) and that which is most downward refracting (August).

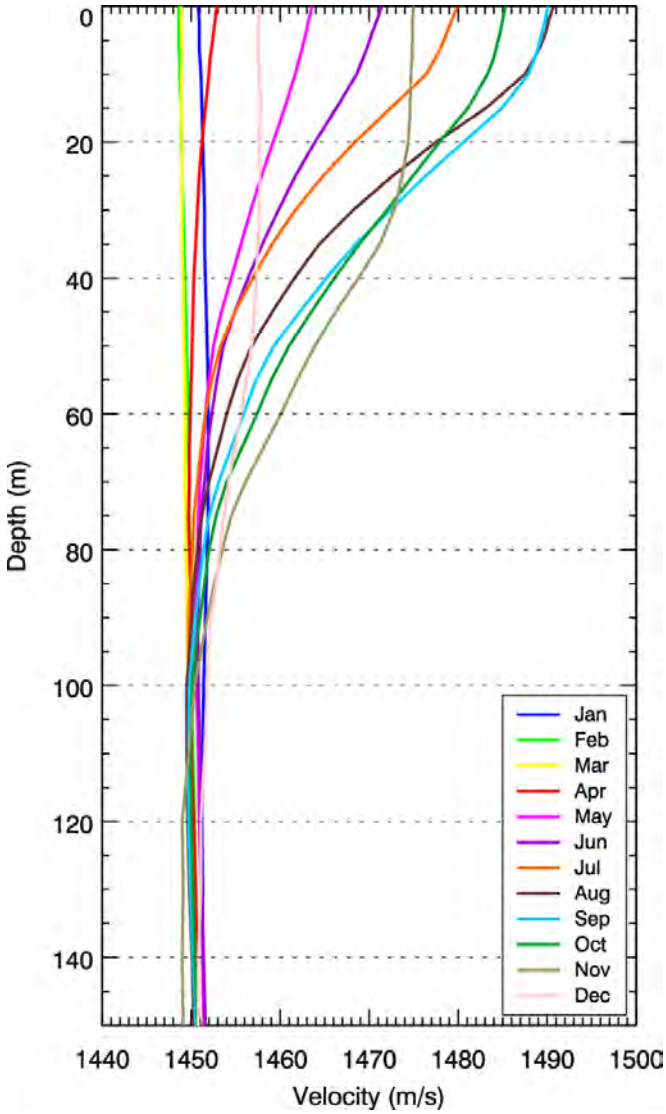

Figure 2-15 Predicted monthly mean sound speed profiles for the nearshore sites: Site A and Corridors 1 and 2

2.4.2 Offshore: White Rose Field

Water depths throughout the White Rose field were obtained from *SRTM30+* (v6.0), a global topography and bathymetry grid with a resolution of 30 arc-seconds or approximately 1 km (Rodriguez et al. 2005). At the studied latitude, the *SRTM30+* grid cell size is approximately 640 × 925 m. The bathymetry data were extracted and re-gridded, using bilinear interpolation, onto a UTM Zone 22 coordinate projection with a horizontal resolution of 500 × 500 m.

The surficial sedimentology in the area of the Jeanne D'Arc Basin, on the northern Grand Banks offshore Newfoundland, has been documented by numerous investigators. The generic geoacoustic profile representing this area (Table 2-9) was developed from information reported by Mosher and Sonnichsen (1992), King and Sonnichsen (2000), Divins (2010) and Abid et al. (2004). The geological stratification is composed of a surficial layer of sand and gravel, which overlays an acoustically-reflective layer of silty to fine sand. It is also characterized by a shallow acoustic basement of unconsolidated tertiary sediment extending for tens of kilometres below the seafloor. Following this profile, the geoacoustic parameters were estimated based on values reported by Ellis and Hughes (1989) and Osler (1994).

Table 2-9 Geoacoustic profile for the White Rose field in Jeanne D'Arc Basin

Sediment	Depth (m)	Density (g/cm^3)	Compressional sound speed (m/s)	Compressional sound attenuation (dB/λ)	Shear sound speed (m/s)	Shear sound attenuation (dB/λ)
Sand and Gravel	0 to 5	1.9 to 2.0	1800 to 1900	0.36 to 0.475	200	3.0
Silty Sand to Fine Sand	5 to 50	1.8 to 2.0	1650 to 1900	0.66 to 0.475		
Sand to Sandy Till	50 to 255	2.0 to 2.1	1900 to 2100	0.475 to 1.0		
Tertiary Bedrock	> 255	2.2	2100	0.21		

Underwater sound speed profiles representing the conditions at the White Rose field were downloaded from the GDEM database (Teague et al. 1990). Temperature-salinity profiles were extracted from the GDEM database and converted to speed of sound in seawater (Figure 2-16; see Section 2.4.1). The sound fields were modelled using two profiles: the most constant sound speed (February); and that which is most downward refracting (August).

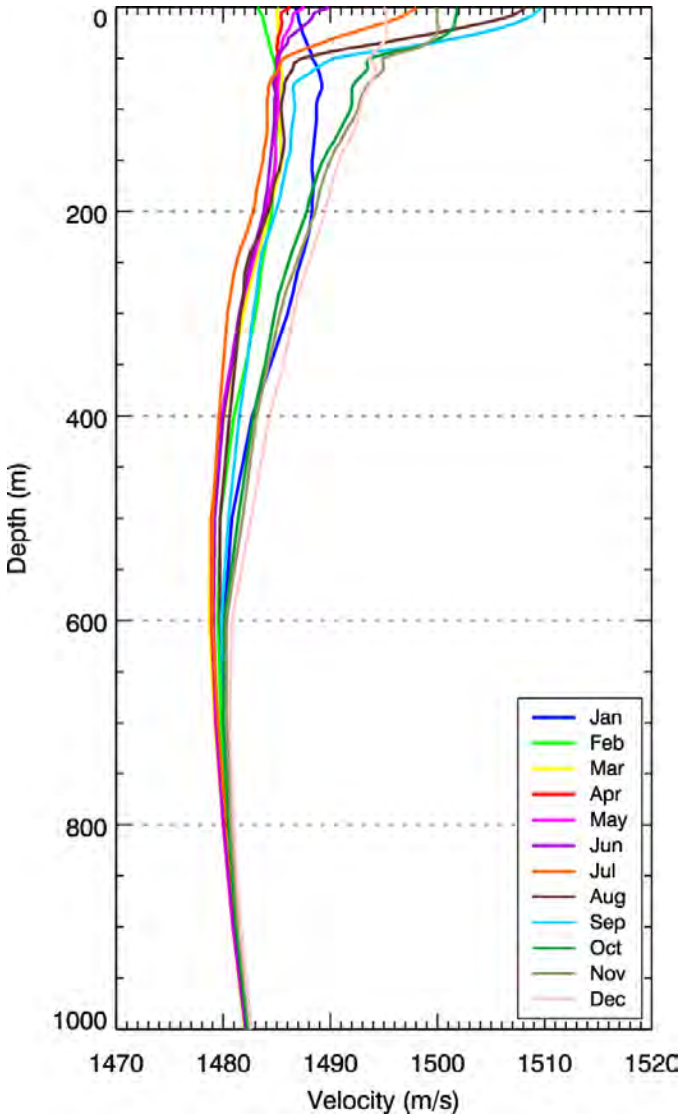

Figure 2-16 Predicted monthly mean sound speed profiles for the offshore site, White Rose field

3.0 Results

The underwater sound fields predicted by the propagation models were sampled such that the received sound level at a surface sampling location is taken as the maximum value occurring over the entire water column. The predicted distances to specific SEL and rms SPL thresholds were computed from these "maximum-over-depth" sound fields. Two distances, relative to the source, are reported for each sound level:

- R_{max}, the maximum range at which the given sound level was encountered in the modelled sound field

- $R_{95\%}$, the maximum range at which the given sound level was encountered after exclusion of the 5 percent farthest such points.

This $R_{95\%}$ definition is meaningful in terms of impact on marine mammals because, regardless of the geometric shape of the noise footprint for a given sound level threshold, $R_{95\%}$ is the predicted range that encompasses at least 95 percent of the animals that could be exposed to sound at or above that level.

The modelled results are presented as tables of R_{max} and $R_{95\%}$ to specified maximum-over-depth SEL (only for impulsive sources (i.e., from blasting activities)) and rms SPL thresholds, and as contour maps of maximum-over-depth sound field showing the directivity in sound propagation. While R_{max} and $R_{95\%}$ are highly relevant, they may vary depending on the location of the source within the modelled area. By considering the distances to the sound level thresholds in combination with the maps of the propagated sound field, better predictions can be made for the variations occurring in realistic scenarios.

3.1 Nearshore: Site A, Corridors 1 and 2

3.1.1 Scenario 1: Site A, Source 1 (Blasting On-shore)

Modelled results for Scenario 1 represent noise from a single blast from 5 kg of pentolite, detonated on land, 20 m below the sea-level (Tables 3-1 to 3-4, Figures 3-1 and 3-2).

Table 3-1 February: Maximum (R_{max}, m) and 95 percent ($R_{95\%}$, m) horizontal distances from an in-ground blast at Site A to modelled maximum-over-depth SEL thresholds with and without M-weighting

SEL (dB re 1 μPa^2·s)	Un-weighted		LFC		MFC		HFC		Pinnipeds	
	R_{max}	$R_{95\%}$	R_{max}	$R_{95\%}$	R_{max}	$R_{95\%}$	R_{max}	$R_{95\%}$	R_{max}	$R_{95\%}$
200	150	144	150	144	–	–	–	–	–	–
190	1 230	922	1 220	861	192	178	149	142	364	320
180	2 800	2 390	2 780	2 380	1 700	1 460	1 390	503	2 110	1 850
170	4 520	3 620	4 520	3 620	4 140	2 830	3 430	2 440	4 490	3 490
160	5 130	4 510	5 090	4 490	4 750	3 860	4 550	3 830	4 780	3 880
150	6 000	5 430	5 940	5 170	5 670	4 330	4 850	4 030	5 930	4 980
140	25 600	18 500	25 500	17 400	6 550	5 230	6 310	5 210	6 630	5 250
130	34 300	28 800	32 800	28 000	7 080	5 460	7 070	5 460	7 130	5 360
120	51 400	37 700	50 400	36 200	35 900	6 620	35 900	6 940	35 900	14 300

Table 3-2 February: Maximum (R_{max}, m) and 95 percent ($R_{95\%}$, m) horizontal distances from an in-ground blast at Site A to modelled maximum-over-depth rms SPL thresholds with and without M-weighting

rms SPL (dB re 1 μPa)	Un-weighted		LFC		MFC		HFC		Pinnipeds	
	R_{max}	$R_{95\%}$	R_{max}	$R_{95\%}$	R_{max}	$R_{95\%}$	R_{max}	$R_{95\%}$	R_{max}	$R_{95\%}$
210	313	282	313	277	–	–	–	–	157	151
200	1 000	894	990	865	286	264	220	210	457	409
190	2 330	1 950	2 230	1 920	1 410	1 270	701	606	1 860	1 580
180	3 290	2 770	3 240	2 760	2 470	2 070	2 140	1 870	2 760	2 420
170	4 530	3 580	4 530	3 580	4 460	3 340	3 740	3 190	4 520	3 550
160	5 290	4 530	5 270	4 520	4 770	3 830	4 700	3 800	4 780	3 820
150	15 300	5 660	5 970	5 330	5 920	4 460	5 590	4 040	5 940	4 990
140	30 100	19 000	25 600	18 100	6 630	5 240	6 580	5 220	6 710	5 230
130	34 500	29 300	34 200	28 600	7 160	5 450	7 130	5 440	7 630	5 360
120	54 100	38 400	51 400	37 400	35 900	6 600	35 900	6 890	35 900	15 300

Table 3-3 August: Maximum (R_{max}, m) and 95 percent ($R_{95\%}$, m) horizontal distances from an in-ground blast at Site A to modelled maximum-over-depth SEL thresholds with and without M-weighting

SEL (dB re 1 μPa^2·s)	Un-weighted		LFC		MFC		HFC		Pinnipeds	
	R_{max}	$R_{95\%}$	R_{max}	$R_{95\%}$	R_{max}	$R_{95\%}$	R_{max}	$R_{95\%}$	R_{max}	$R_{95\%}$
200	130	130	130	128	–	–	–	–	–	–
190	1 030	886	1 010	840	184	175	144	139	348	311
180	2 730	2 330	2 720	2 320	1 560	1 380	623	559	2 060	1 810
170	4 520	3 620	4 520	3 620	3 640	2 590	2 780	2 350	4 480	3 410
160	4 980	4 420	4 940	4 390	4 800	3 870	4 770	3 820	4 840	3 900
150	6 020	5 380	5 780	5 120	4 890	4 020	4 890	4 070	5 580	4 820
140	25 500	17 900	20 600	17 000	6 100	5 180	6 070	5 150	6 460	5 190
130	34 100	28 400	32 700	27 300	7 000	5 470	6 970	5 470	7 020	5 350
120	50 400	36 700	50 400	34 900	35 900	5 900	35 900	5 890	35 900	13 800

Table 3-4 August: Maximum (R_{max}, m) and 95 percent ($R_{95\%}$, m) horizontal distances from an in-ground blast at Site A to modelled maximum-over-depth rms SPL thresholds with and without M-weighting

rms SPL (dB re 1 μPa)	Un-weighted		LFC		MFC		HFC		Pinnipeds	
	R_{max}	$R_{95\%}$	R_{max}	$R_{95\%}$	R_{max}	$R_{95\%}$	R_{max}	$R_{95\%}$	R_{max}	$R_{95\%}$
210	289	270	286	263	–	–	–	–	150	143
200	1 020	890	933	850	279	256	216	205	451	412
190	2 250	1 890	2 120	1 860	1 350	926	721	640	1 770	1 430
180	3 160	2 720	3 150	2 710	2 210	1 970	2 090	1 830	2 720	2 370
170	4 520	3 570	4 520	3 580	4 180	3 300	3 710	3 040	4 490	3 520
160	5 090	4 440	5 050	4 420	4 840	3 840	4 800	3 810	4 850	3 840
150	15 200	5 590	5 850	5 290	4 890	4 000	4 890	3 960	5 750	4 870
140	30 100	18 600	25 500	17 600	6 470	5 180	6 200	5 150	6 600	5 180
130	34 300	28 800	34 000	28 200	7 050	5 440	7 020	5 450	7 070	5 310
120	50 400	37 700	50 400	36 400	35 900	5 970	35 900	6 010	35 900	15 000

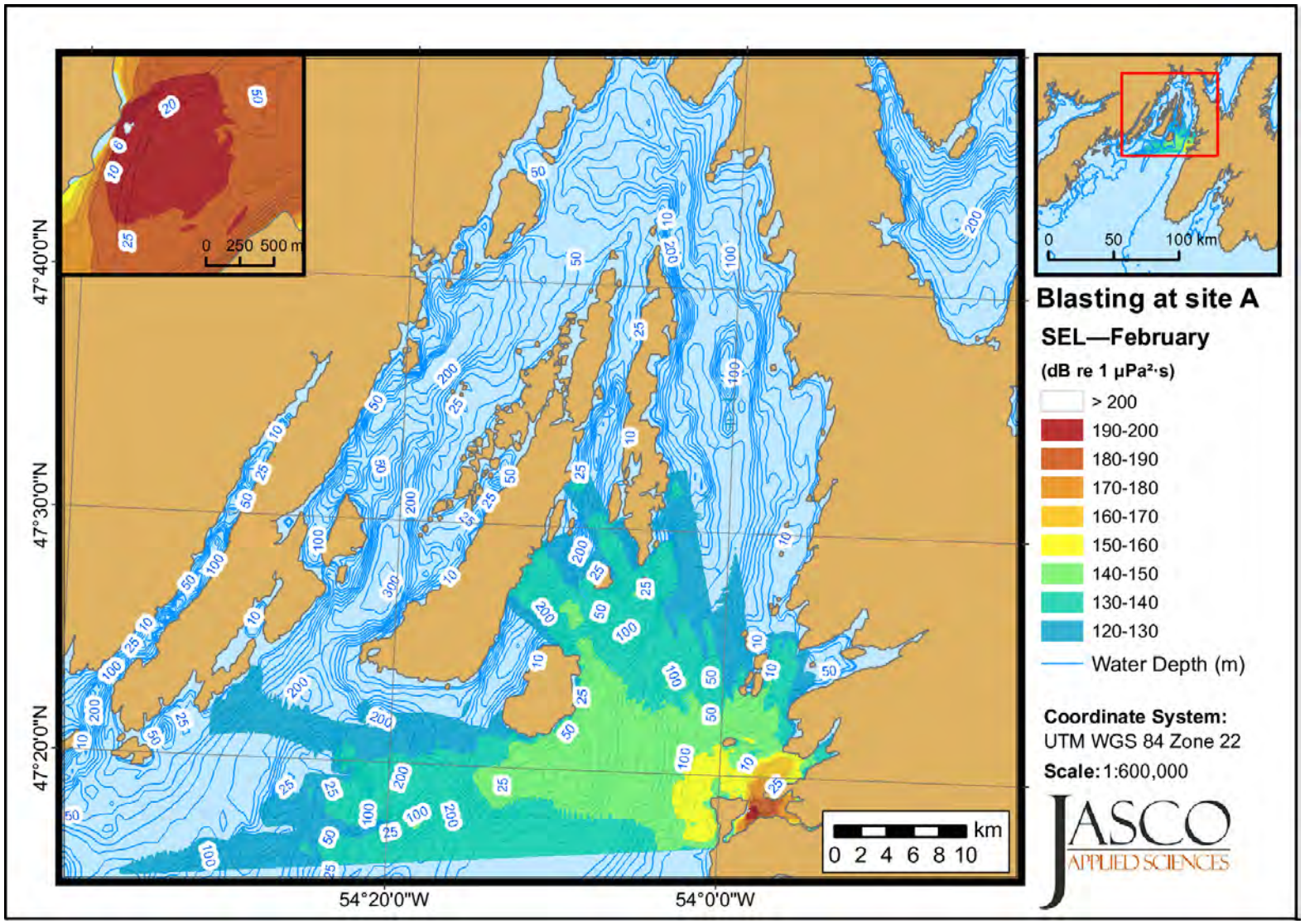

Figure 3-1 February: Received maximum-over-depth sound levels from an in-ground blast at Site A

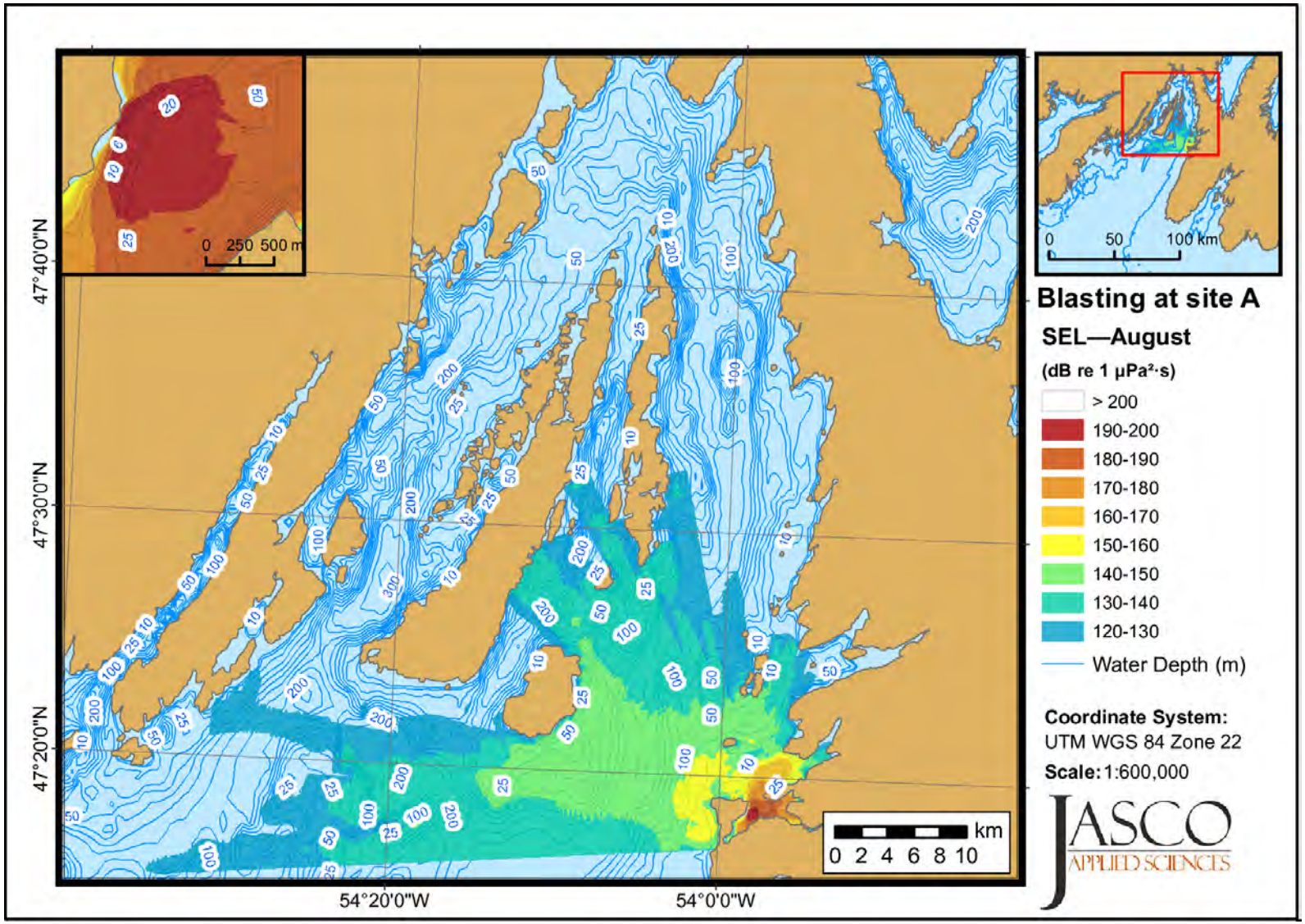

Figure 3-2 August: Received maximum-over-depth sound levels from an in-ground blast at Site A

3.1.2 Scenario 2: Site A, Source 3 (Cutter Suction Dredge)

Modelled results for Scenario 2 represent (continuous) noise from a cutter suction dredge operating at Site A (Tables 3-5 and 3-6, Figures 3-3 and 3-4).

Table 3-5 February: Maximum (R_{max}, m) and 95 percent ($R_{95\%}$, m) horizontal distances from the cutter suction dredge at Site A to modelled maximum-over-depth sound level thresholds with and without M-weighting

rms SPL (dB re 1 µPa)	Un-weighted		LFC		MFC		HFC		Pinnipeds	
	R_{max}	$R_{95\%}$	R_{max}	$R_{95\%}$	R_{max}	$R_{95\%}$	R_{max}	$R_{95\%}$	R_{max}	$R_{95\%}$
190	–	–	–	–	–	–	–	–	–	–
180	< 5	< 5	< 5	< 5	< 5	< 5	< 5	< 5	< 5	< 5
170	22	22	22	22	16	16	14	14	21	21
160	163	139	160	136	112	97	110	90	140	117
150	1 357	1 109	1 311	1 087	706	515	692	476	1 165	616
140	3 530	2 598	3 530	2 515	3 528	2 115	3 259	2 063	3 530	2 293
130	8 375	5 506	8 371	5 480	8 371	5 428	7 939	5 383	8 375	5 480
120	15 991	13 777	15 991	13 768	15 991	13 707	15 991	13 651	15 991	13 762

Table 3-6 August: Maximum (R_{max}, m) and 95 percent ($R_{95\%}$, m) horizontal distances from the cutter suction dredge at Site A to modelled maximum-over-depth sound level thresholds with and without M-weighting

rms SPL (dB re 1 µPa)	Un-weighted		LFC		MFC		HFC		Pinnipeds	
	R_{max}	$R_{95\%}$	R_{max}	$R_{95\%}$	R_{max}	$R_{95\%}$	R_{max}	$R_{95\%}$	R_{max}	$R_{95\%}$
190	–	–	–	–	–	–	–	–	–	–
180	< 5	< 5	< 5	< 5	< 5	< 5	< 5	< 5	< 5	< 5
170	22	22	22	21	14	14	14	11	20	18
160	160	125	160	121	105	92	100	86	135	106
150	863	635	862	616	601	471	526	435	740	546
140	2 509	2 027	2 503	2 022	2 370	1 900	2 309	1 872	2 443	1 970
130	5 698	4 931	5 698	4 934	5 624	4 775	5 624	4 494	5 679	4 888
120	8 371	6 629	8 371	6 627	8 371	6 396	8 371	6 258	8 371	6 569

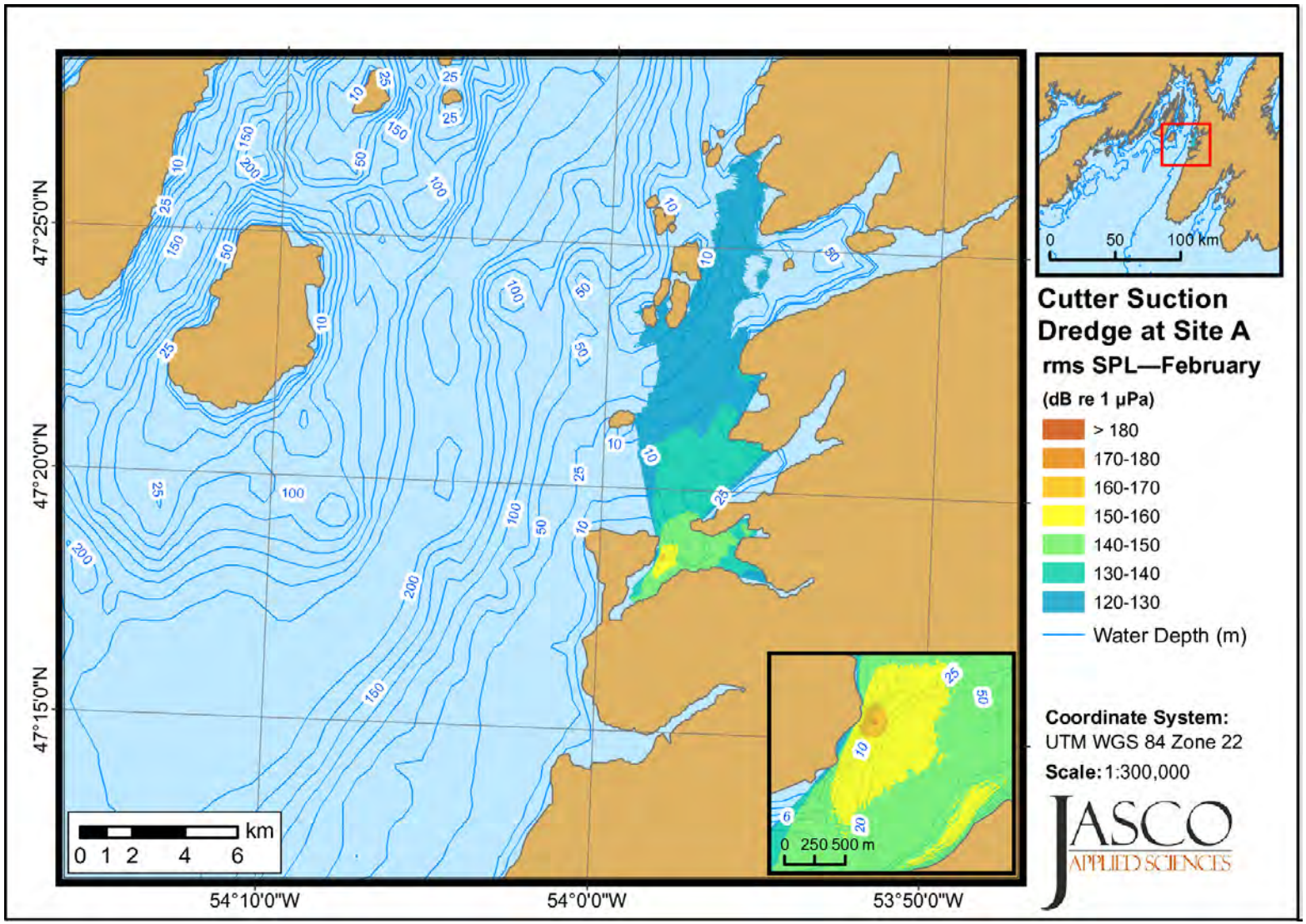

Figure 3-3 February: Received maximum-over-depth sound levels from the cutter suction dredge at Site A

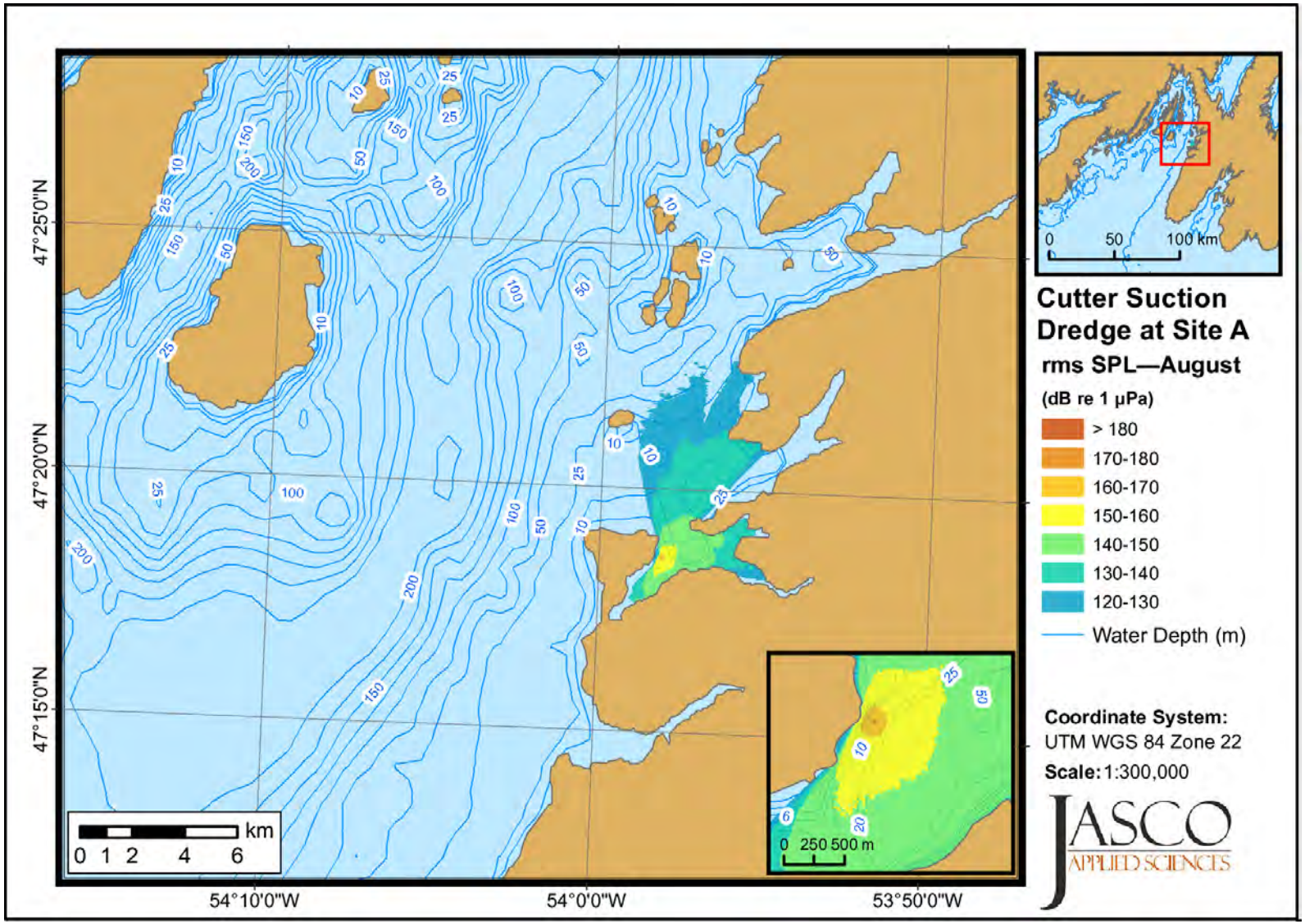

Figure 3-4 August: Received maximum-over-depth sound levels from the cutter suction dredge at Site A

3.1.3 Scenario 3: Corridor 1, Source 2 (Blasting in Water)

Modelled results for Scenario 3 represent noise from a single blast from 5 kg of pentolite, detonated at 2 m below the seafloor (Tables 3-7 to 3-10; Figures 3-5 and 3-6).

Table 3-7 February: Maximum (R_{max}, m) and 95 percent ($R_{95\%}$, m) horizontal distances from an in-ground blast at Corridor 1 to modelled maximum-over-depth SEL thresholds with and without M-weighting

SEL (dB re 1 µPa^2·s)	Un-weighted		LFC		MFC		HFC		Pinnipeds	
	R_{max}	$R_{95\%}$	R_{max}	$R_{95\%}$	R_{max}	$R_{95\%}$	R_{max}	$R_{95\%}$	R_{max}	$R_{95\%}$
220	13	13	13	13	–	–	–	–	–	–
210	84	78	84	76	25	24	24	24	34	34
200	512	442	504	425	84	79	70	66	164	141
190	2 250	1 540	2 250	1 520	387	346	317	278	701	578
180	4 240	3 180	4 230	3 140	1 980	1 500	1 620	1 090	2 760	2 060
170	4 620	3 680	4 620	3 680	3 810	2 840	3 380	2 590	4 460	3 550
160	8 510	5 000	8 500	4 950	4 850	3 980	4 810	3 830	5 030	4 320
150	21 100	10 900	21 100	10 800	11 300	8 210	11 200	8 070	18 800	8 780
140	37 500	24 500	37 500	24 500	37 500	24 200	37 500	24 000	37 500	24 400
130	58 800	52 000	58 800	52 100	58 800	52 400	58 800	52 400	58 800	52 400
120	62 700	51 700	62 700	51 800	62 700	52 100	62 300	52 200	62 700	52 100

Table 3-8 February: Maximum (R_{max}, m) and 95 percent ($R_{95\%}$, m) horizontal distances from an in-ground blast at Corridor 1 to modelled maximum-over-depth rms SPL thresholds with and without M-weighting

rms SPL (dB re 1 µPa)	Un-weighted		LFC		MFC		HFC		Pinnipeds	
	R_{max}	$R_{95\%}$	R_{max}	$R_{95\%}$	R_{max}	$R_{95\%}$	R_{max}	$R_{95\%}$	R_{max}	$R_{95\%}$
230	42	38	38	37	–	–	–	–	12	12
220	217	199	208	193	43	41	40	38	70	64
210	708	614	692	603	182	168	141	130	320	281
200	1 900	1 420	1 890	1 410	608	503	495	430	847	735
190	3 230	2 610	3 220	2 600	1 690	1 310	1 390	1 070	2 350	1 650
180	4 460	3 530	4 460	3 520	3 110	2 370	2 820	2 180	3 760	2 920
170	4 810	4 040	4 810	4 030	4 470	3 610	4 390	3 520	4 650	3 740
160	8 740	7 300	8 730	7 270	6 380	4 610	5 200	4 480	8 510	4 870
150	25 200	18 100	25 200	17 900	21 300	10 600	21 300	9 140	24 900	12 600
140	54 900	28 700	54 900	28 700	54 900	27 200	54 900	26 600	54 900	28 100
130	58 800	51 500	58 800	51 600	58 800	52 000	58 800	52 000	58 800	52 000
120	63 100	51 200	63 100	51 200	63 100	51 600	63 100	51 600	63 100	51 600

Table 3-9 August: Maximum (R_{max}, m) and 95 percent ($R_{95\%}$, m) horizontal distances from an in-ground blast at Corridor 1 to modelled maximum-over-depth SEL thresholds with and without M-weighting

SEL (dB re 1 µPa^2·s)	Un-weighted		LFC		MFC		HFC		Pinnipeds	
	R_{max}	$R_{95\%}$	R_{max}	$R_{95\%}$	R_{max}	$R_{95\%}$	R_{max}	$R_{95\%}$	R_{max}	$R_{95\%}$
220	12	12	12	12	–	–	–	–	–	–
210	80	71	76	70	25	25	24	24	34	33
200	445	402	437	394	80	76	68	62	155	134
190	2 100	1 500	2 080	1 480	388	337	341	263	652	553
180	4 040	2 970	4 030	2 930	1 880	1 440	1 550	984	2 670	2 000
170	4 520	3 620	4 520	3 620	3 370	2 690	3 220	2 410	4 380	3 470
160	8 010	4 730	8 000	4 710	4 820	3 850	4 670	3 730	4 950	4 200
150	11 800	9 480	11 800	9 420	9 650	7 780	9 510	7 490	11 400	8 160
140	29 700	20 600	29 700	20 600	29 700	18 100	29 700	17 700	29 700	18 800
130	50 400	28 100	50 400	28 000	50 400	25 300	50 400	24 900	50 400	25 900
120	56 500	42 900	56 500	42 900	56 500	44 300	56 500	44 200	56 500	44 400

Table 3-10 August: Maximum (R_{max}, m) and 95 percent ($R9_{5\%}$, m) horizontal distances from an in-ground blast at Corridor 1 to modelled maximum-over-depth rms SPL thresholds with and without M-weighting

rms SPL (dB re 1 µPa)	Un-weighted		LFC		MFC		HFC		Pinnipeds	
	R_{max}	$R_{95\%}$	R_{max}	$R_{95\%}$	R_{max}	$R_{95\%}$	R_{max}	$R_{95\%}$	R_{max}	$R_{95\%}$
230	38	37	37	35	–	–	–	–	12	12
220	200	183	195	176	42	40	40	38	69	62
210	647	587	641	578	178	159	146	127	341	269
200	1 820	1 390	1 810	1 380	604	496	482	420	831	720
190	3 200	2 540	3 180	2 510	1 630	1 280	1 360	1 050	2 230	1 610
180	4 420	3 480	4 400	3 480	2 870	2 290	2 740	2 110	3 340	2 810
170	4 770	3 950	4 770	3 940	4 400	3 520	4 050	3 380	4 590	3 670
160	8 410	5 570	8 410	5 500	5 220	4 550	4 980	4 400	5 580	4 770
150	19 200	10 700	19 200	10 600	11 500	8 550	11 100	8 140	12 100	9 520
140	33 700	21 800	33 700	21 800	29 700	20 000	29 700	19 400	33 700	20 700
130	51 700	33 500	51 100	33 600	51 000	32 500	51 000	31 900	51 000	33 200
120	57 700	44 000	57 700	44 100	57 600	45 200	57 600	45 200	57 600	45 300

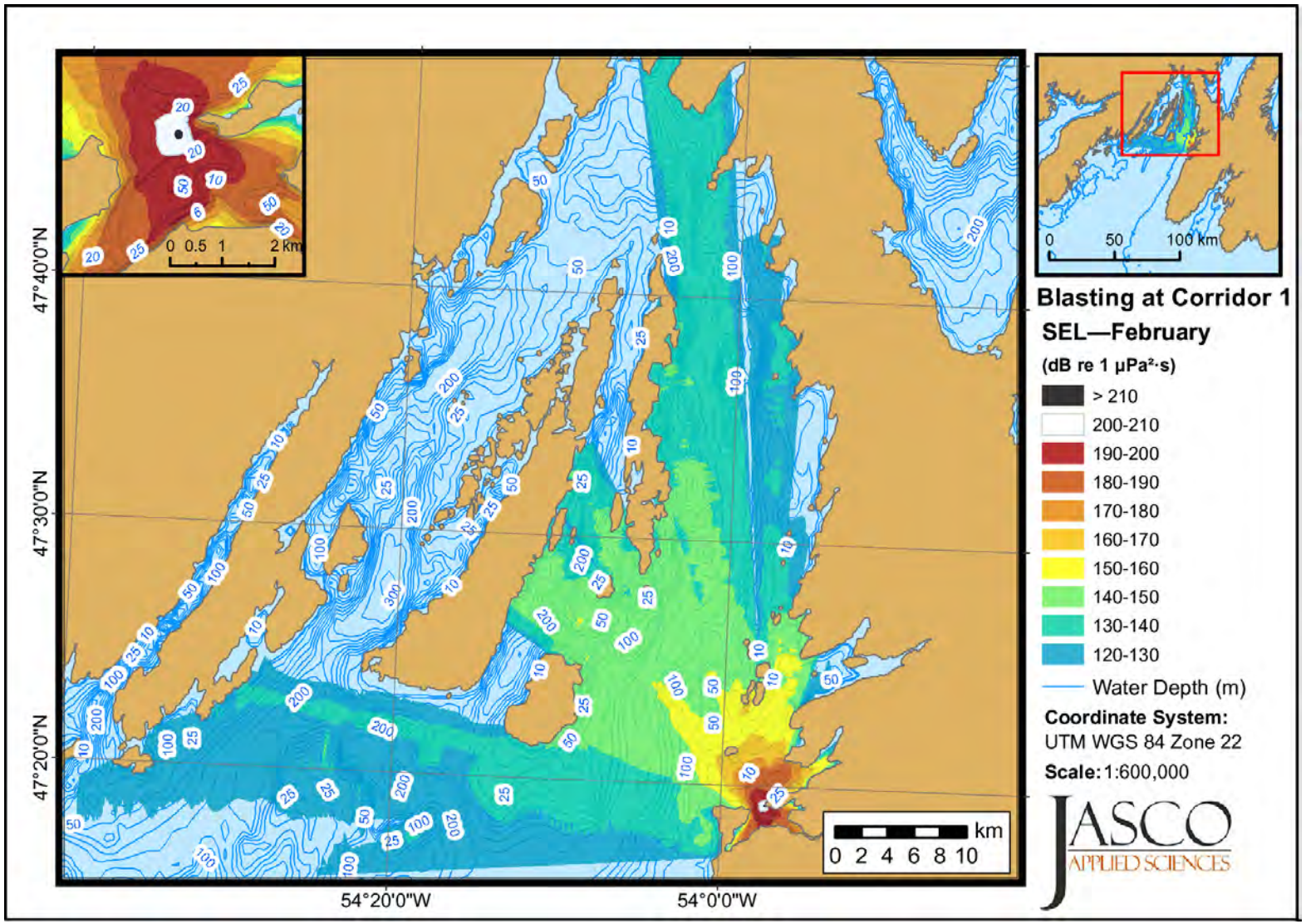

Figure 3-5 February: Received maximum-over-depth sound levels from an in-water blast at Corridor 1

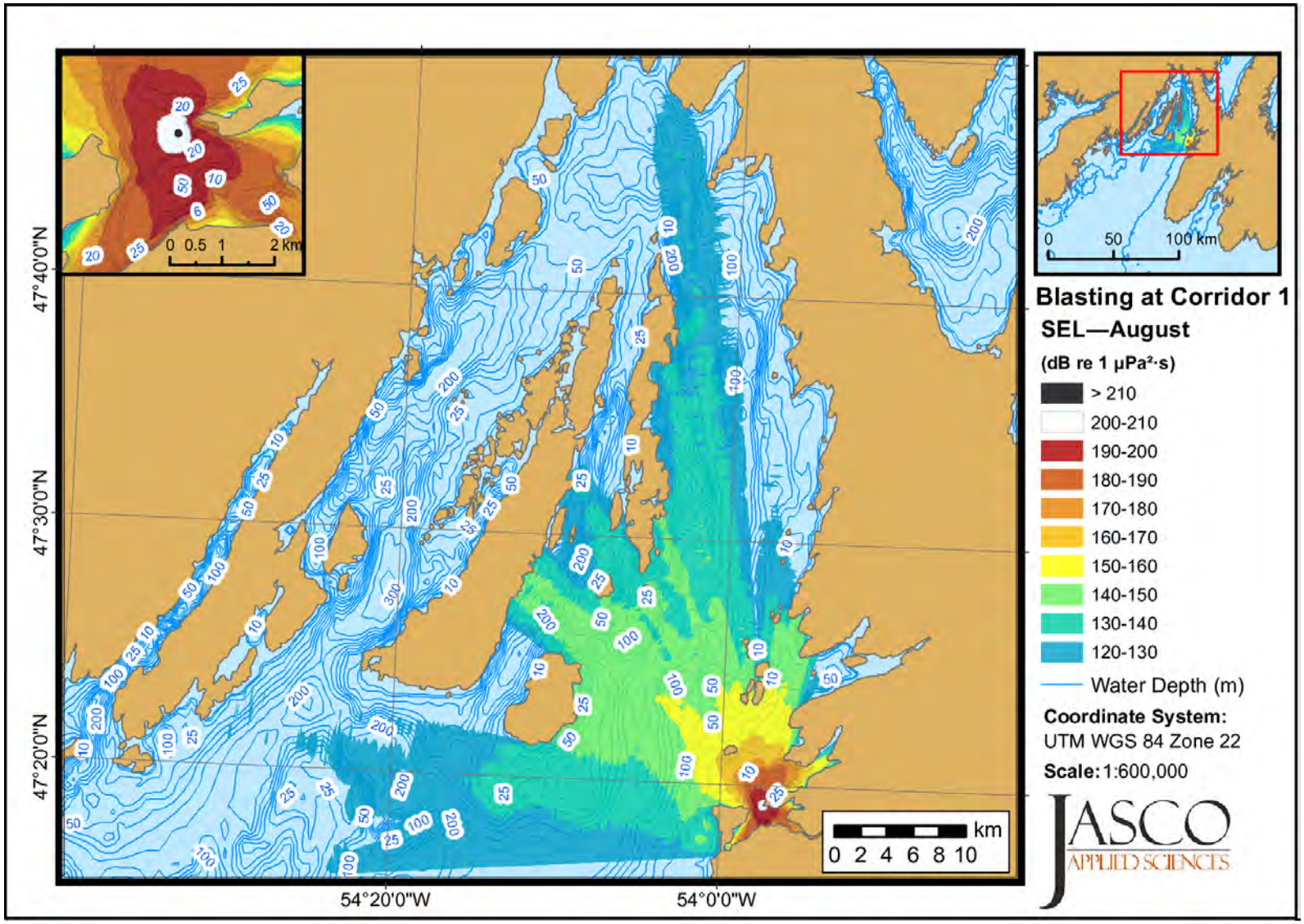

Figure 3-6 August: Received maximum-over-depth sound levels from an in-water blast at Corridor 1

3.1.4 Scenario 4: Corridor 1, Source 4 (Trailing Suction Hopper Dredge)

Modelled results for Scenario 4 represent (continuous) noise from a trailing suction hopper dredge operating in the southern section of Corridor 1 (Tables 3-11 and 3-12; Figures 3-7 and 3-8).

Table 3-11 February: Maximum (R_{max}, m) and 95 percent ($R_{95\%}$, m) horizontal distances from the trailing suction hopper dredge at Corridor 1 to modelled maximum-over-depth sound level thresholds with and without M-weighting

rms SPL (dB re 1 µPa)	Un-weighted		LFC		MFC		HFC		Pinnipeds	
	R_{max}	$R_{95\%}$	R_{max}	$R_{95\%}$	R_{max}	$R_{95\%}$	R_{max}	$R_{95\%}$	R_{max}	$R_{95\%}$
190	< 5	< 5	< 5	< 5	–	–	–	–	–	–
180	7	7	7	7	< 5	< 5	< 5	< 5	< 5	< 5
170	45	43	43	42	16	16	15	14	27	25
160	284	248	282	244	125	111	115	96	180	154
150	1 546	988	1 505	977	802	631	676	559	945	792
140	3 942	3 236	3 941	3 216	3 836	2 878	3 794	2 748	3 939	3 108
130	8 779	5 056	8 776	4 973	8 776	4 807	8 776	4 735	8 776	4 947
120	24 927	18 239	24 925	18 242	24 886	17 751	24 884	17 344	24 925	18 114

Table 3-12 August: Maximum (R_{max}, m) and 95 percent ($R_{95\%}$, m) horizontal distances from the trailing suction hopper dredge at Corridor 1 to modelled maximum-over-depth sound level thresholds with and without M-weighting

rms SPL (dB re 1 µPa)	Un-weighted		LFC		MFC		HFC		Pinnipeds	
	R_{max}	$R_{95\%}$	R_{max}	$R_{95\%}$	R_{max}	$R_{95\%}$	R_{max}	$R_{95\%}$	R_{max}	$R_{95\%}$
190	< 5	< 5	< 5	< 5	–	–	–	–	–	–
180	7	7	7	7	< 5	< 5	< 5	< 5	< 5	< 5
170	43	40	41	40	16	16	15	14	25	25
160	270	236	265	234	119	107	99	91	176	150
150	1 067	924	1 041	913	725	583	641	515	890	731
140	3 135	2 635	3 122	2 628	2 610	1 879	2 444	1 740	2 965	2 341
130	4 804	3 997	4 804	3 982	4 768	3 768	4 743	3 688	4 801	3 906
120	11 623	7 163	11 623	7 149	11 075	6 456	11 072	6 219	11 607	6 909

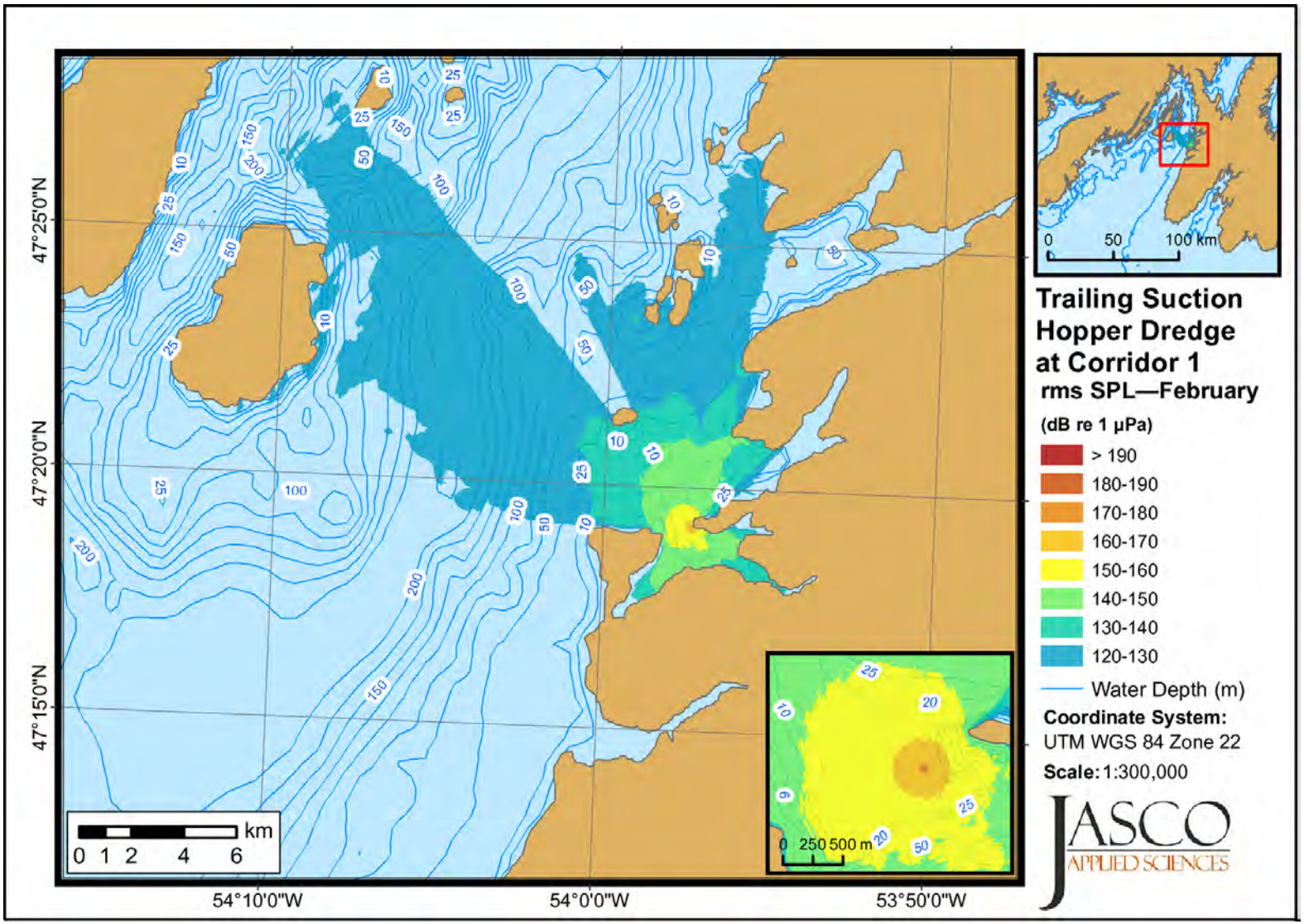

Figure 3-7 February: Received maximum-over-depth sound levels from the trailing suction hopper dredge at Corridor 1

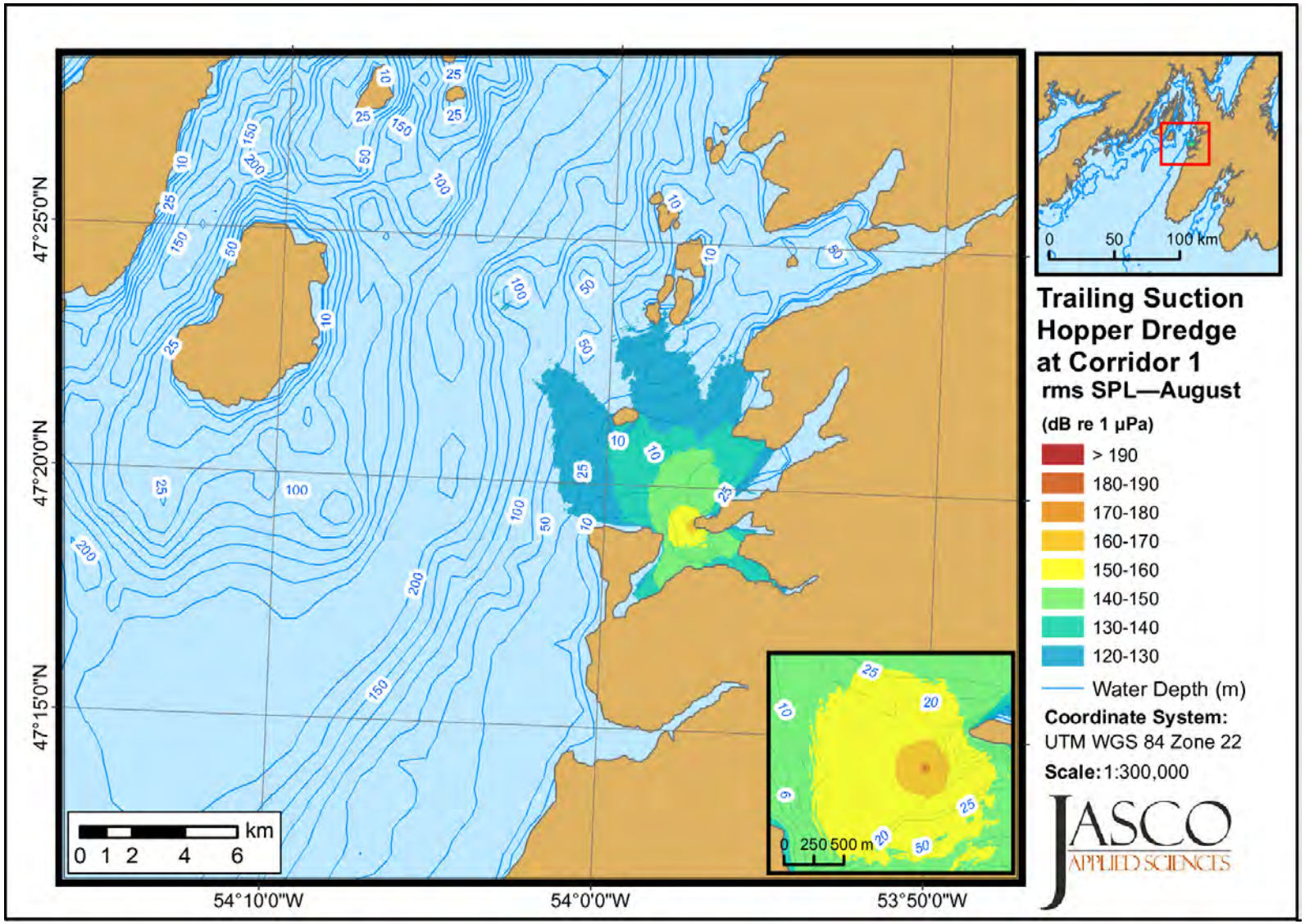

Figure 3-8 August: Received maximum-over-depth sound levels from the trailing suction hopper dredge at Corridor 1

3.1.5 Scenario 5: Corridor 2, Source 4 (Trailing Suction Hopper Dredge)

Modelled results for Scenario 5 represent (continuous) noise from a trailing suction hopper dredge operating in the eastern section of Corridor 2 (Tables 3-13 and 3-14; Figures 3-9 and 3-10).

Table 3-13 February: Maximum (R_{max}, m) and 95 percent ($R_{95\%}$, m) horizontal distances from the trailing suction hopper dredge at Corridor 2 to modelled maximum-over-depth sound level thresholds with and without M-weighting

rms SPL (dB re 1 µPa)	Un-weighted		LFC		MFC		HFC		Pinnipeds	
	R_{max}	$R_{95\%}$	R_{max}	$R_{95\%}$	R_{max}	$R_{95\%}$	R_{max}	$R_{95\%}$	R_{max}	$R_{95\%}$
190	< 5	< 5	< 5	< 5	–	–	–	–	–	–
180	7	7	7	7	< 5	< 5	< 5	< 5	< 5	< 5
170	45	43	43	43	18	18	16	16	30	29
160	290	248	290	244	130	110	115	97	185	159
150	1 191	928	1 191	911	701	574	658	523	884	693
140	4 483	3 047	4 299	3 041	3 541	2 833	3 533	2 715	3 691	3 007
130	7 677	5 364	7 677	5 302	7 587	5 158	7 587	5 070	7 656	5 266
120	23 686	19 775	23 662	19 674	22 970	18 903	22 023	18 586	23 583	19 421

Table 3-14 August: Maximum (R_{max}, m) and 95 percent ($R_{95\%}$, m) horizontal distances from the trailing suction hopper dredge at Corridor 2 to modelled maximum-over-depth sound level thresholds with and without M-weighting

rms SPL (dB re 1 µPa)	Un-weighted		LFC		MFC		HFC		Pinnipeds	
	R_{max}	$R_{95\%}$	R_{max}	$R_{95\%}$	R_{max}	$R_{95\%}$	R_{max}	$R_{95\%}$	R_{max}	$R_{95\%}$
190	< 5	< 5	< 5	< 5	–	–	–	–	–	–
180	7	7	7	7	< 5	< 5	< 5	< 5	< 5	< 5
170	43	41	42	40	18	16	14	14	29	27
160	271	232	266	227	114	105	103	90	172	149
150	1 028	869	1 026	853	636	518	568	474	792	645
140	3 345	2 727	3 345	2 719	2 828	2 166	2 690	2 089	3 156	2 434
130	5 770	4 200	5 770	4 174	5 751	3 816	5 301	3 699	5 768	4 052
120	16 436	7 498	16 426	7 322	15 060	6 376	15 055	6 228	16 241	6 688

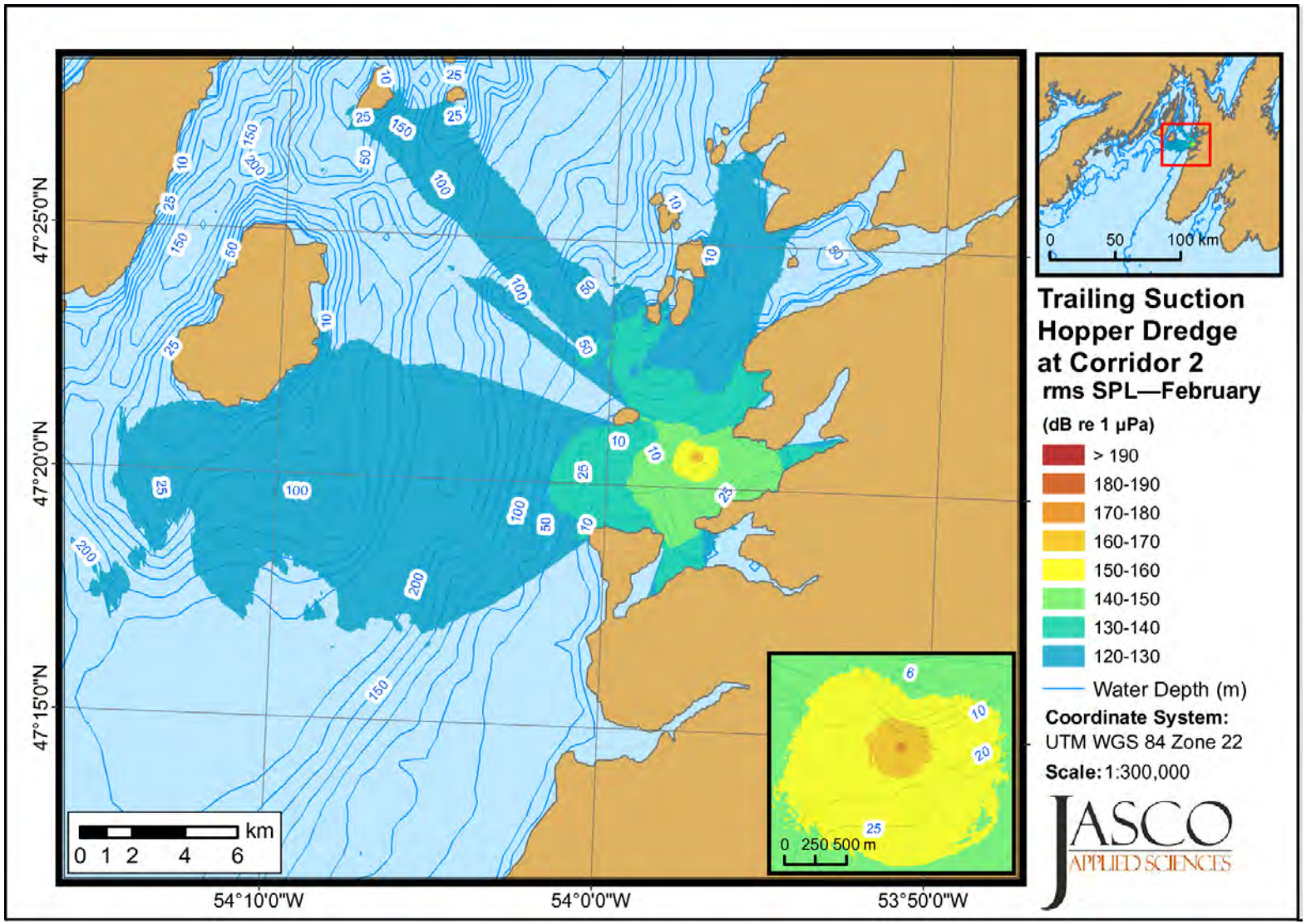

Figure 3-9 February: Received maximum-over-depth sound levels from the trailing suction hopper dredge at Corridor 2

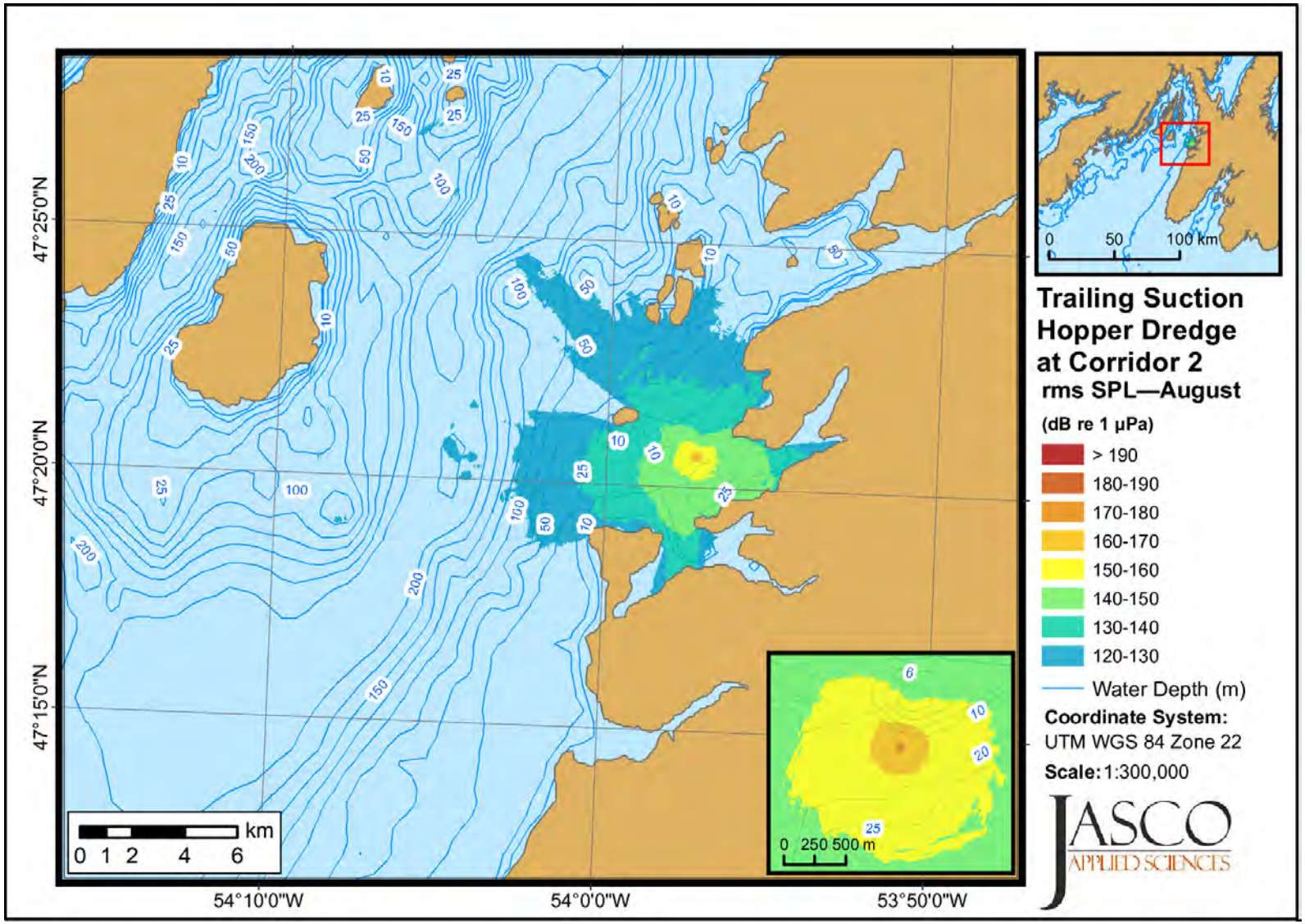

Figure 3-10 August: Received maximum-over-depth sound levels from the trailing suction hopper dredge at Corridor 2

3.2 Offshore: White Rose Field

3.2.1 Scenario 6: White Rose Field, Source 4 (Trailing Suction Hopper Dredge)

Modelled results for Scenario 6 represent (continuous) noise from a trailing suction hopper dredge operating at the White Rose field site (Tables 3-15 and 3-16; Figures 3-11 and 3-12).

Table 3-15 February: Maximum (R_{max}, m) and 95 percent ($R_{95\%}$, m) horizontal distances from the trailing suction hopper dredge at White Rose Field to modelled maximum-over-depth sound level thresholds with and without M-weighting

rms SPL (dB re 1 µPa)	Un-weighted		LFC		MFC		HFC		Pinnipeds	
	R_{max}	$R_{95\%}$	R_{max}	$R_{95\%}$	R_{max}	$R_{95\%}$	R_{max}	$R_{95\%}$	R_{max}	$R_{95\%}$
190	< 5	< 5	< 5	< 5	–	–	–	–	–	–
180	7	7	7	7	< 5	< 5	< 5	< 5	< 5	< 5
170	22	22	22	22	11	11	10	10	16	16
160	95	89	92	89	42	41	36	35	56	54
150	565	461	549	455	250	240	224	216	367	336
140	3 787	2 954	3 691	2 909	2 060	1 563	1 869	1 340	2 698	2 065
130	14 933	12 211	14 933	12 109	11 148	8 715	9 631	8 526	13v678	10 182
120	49 604	39 812	49 600	39 328	49 600	34 491	48 165	33 747	49 600	37 250

Table 3-16 August: Maximum (R_{max}, m) and 95 percent ($R_{95\%}$, m) horizontal distances from the trailing suction hopper dredge at White Rose Field to modelled maximum-over-depth sound level thresholds with and without M-weighting

rms SPL (dB re 1 µPa)	Un-weighted		LFC		MFC		HFC		Pinnipeds	
	R_{max}	$R_{95\%}$	R_{max}	$R_{95\%}$	R_{max}	$R_{95\%}$	R_{max}	$R_{95\%}$	R_{max}	$R_{95\%}$
190	< 5	< 5	< 5	< 5	–	–	–	–	–	–
180	7	7	7	7	< 5	< 5	< 5	< 5	< 5	< 5
170	22	22	22	22	11	11	11	11	16	16
160	95	90	93	89	41	40	36	36	55	54
150	546	485	545	457	271	258	240	209	390	354
140	3 801	2 864	3 780	2 824	2 414	1 635	1 852	1 490	3 126	2 184
130	13 957	10 989	13 909	10 917	10 523	8 419	10 338	7 632	12 462	9 622
120	37 346	28 189	37 346	28 022	32 294	23 825	30 270	22 726	33 591	26 120

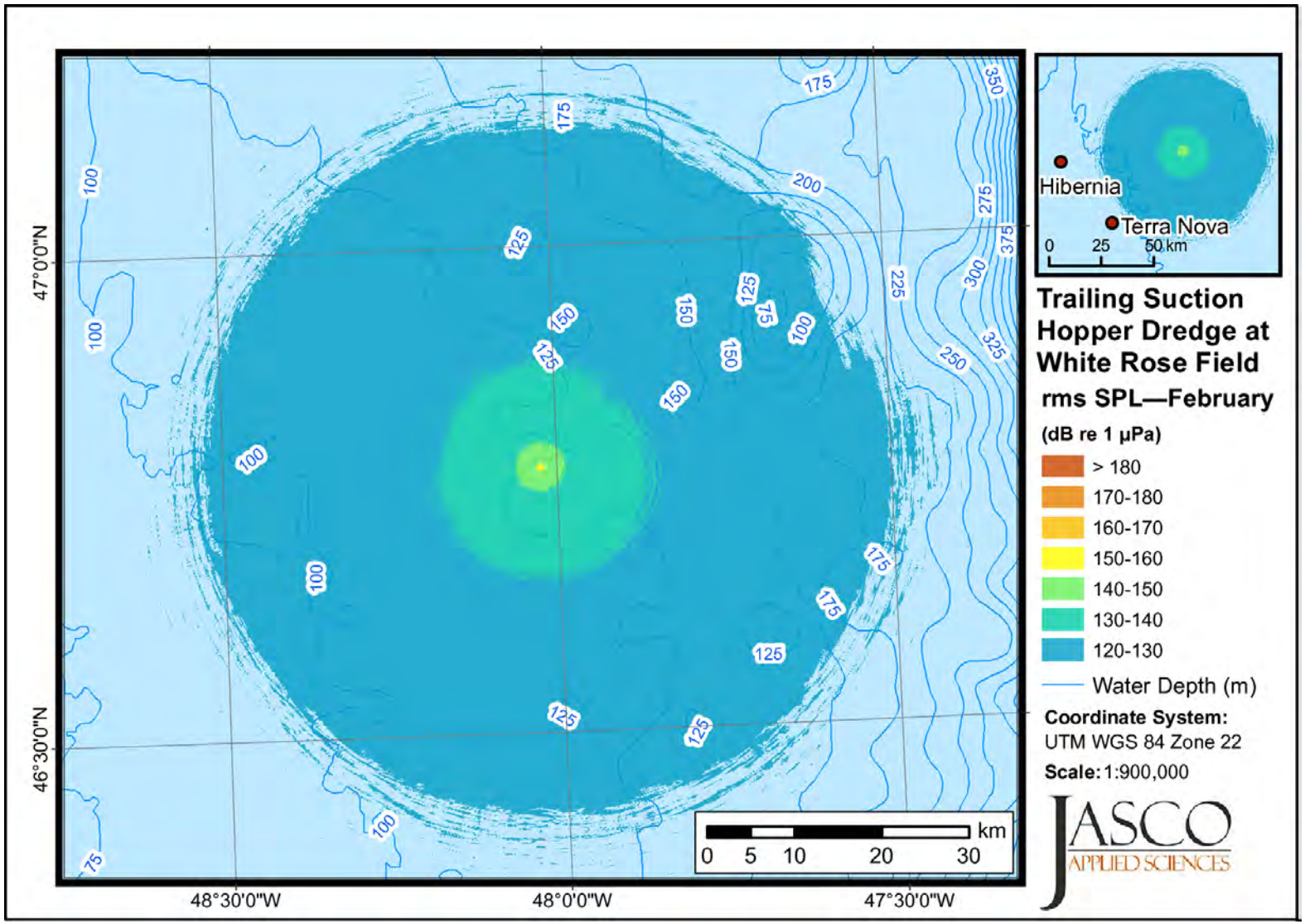

Figure 3-11 February: Received maximum-over-depth sound levels from the trailing suction hopper dredge at White Rose Field

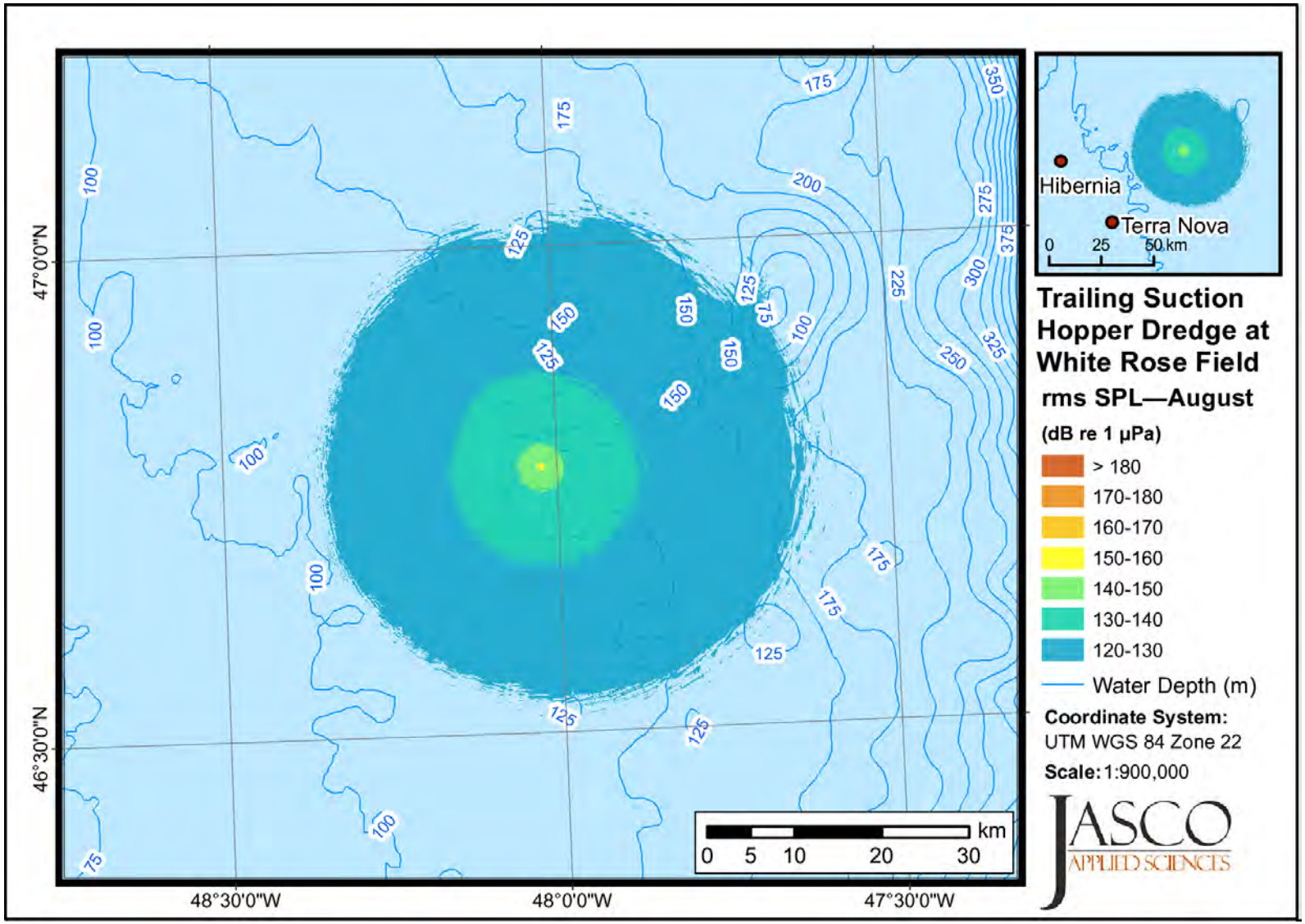

Figure 3-12 August: Received maximum-over-depth sound levels from the trailing suction hopper dredge at White Rose Field

3.2.2 Scenario 7: White Rose Field, Source 5 (Drilling Wellhead Platform)

Modelled results for Scenario 7 represent (continuous) noise from the drilling operations at the White Rose field (Tables 3-17 and 3-18; Figures 3-13 and 3-14).

Table 3-17 February: Maximum (R_{max}, m) and 95 percent ($R_{95\%}$, m) horizontal distances from the drilling platform at White Rose Field to modelled maximum-over-depth sound level thresholds with and without M-weighting

rms SPL (dB re 1 µPa)	Un-weighted		LFC		MFC		HFC		Pinnipeds	
	R_{max}	$R_{95\%}$	R_{max}	$R_{95\%}$	R_{max}	$R_{95\%}$	R_{max}	$R_{95\%}$	R_{max}	$R_{95\%}$
170	–	–	–	–	–	–	–	–	–	–
160	< 5	< 5	< 5	< 5	–	–	–	–	–	–
150	7	7	7	7	< 5	< 5	< 5	< 5	< 5	< 5
140	18	18	18	18	7	7	7	7	11	11
130	97	95	96	94	32	32	29	29	47	47
120	720	584	699	565	205	178	145	139	306	266

Table 3-18 August: Maximum (R_{max}, m) and 95 percent ($R_{95\%}$, m) horizontal distances from the drilling platform at White Rose Field to modelled maximum-over-depth sound level thresholds with and without M-weighting

rms SPL (dB re 1 µPa)	Un-weighted		LFC		MFC		HFC		Pinnipeds	
	R_{max}	$R_{95\%}$	R_{max}	$R_{95\%}$	R_{max}	$R_{95\%}$	R_{max}	$R_{95\%}$	R_{max}	$R_{95\%}$
170	–	–	–	–	–	–	–	–	–	–
160	< 5	< 5	< 5	< 5	–	–	–	–	–	–
150	7	7	7	7	< 5	< 5	< 5	< 5	< 5	< 5
140	18	18	18	18	7	7	7	7	11	11
130	97	94	96	93	32	32	30	29	51	50
120	858	677	850	666	186	173	155	139	326	297

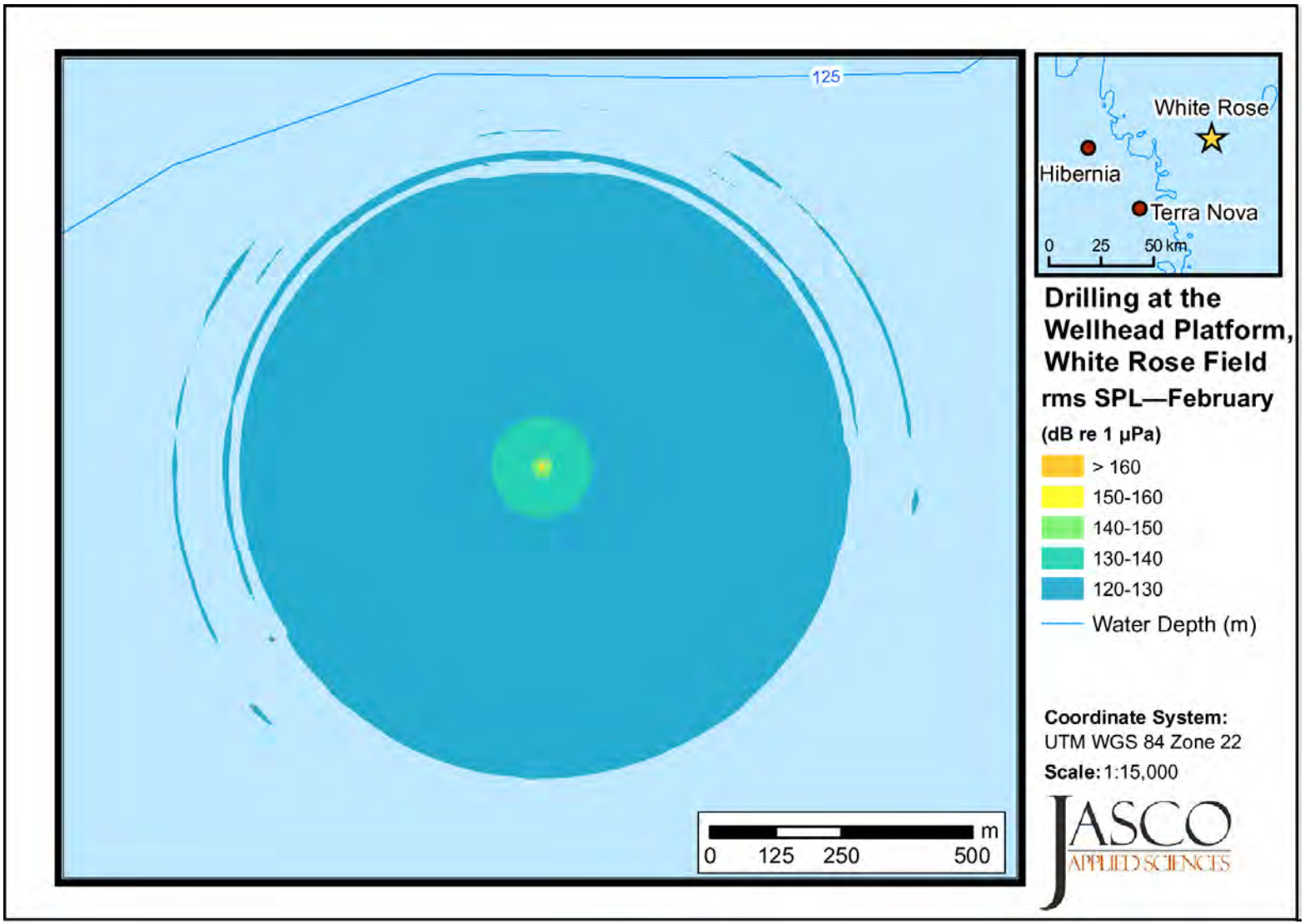

Figure 3-13 February: Received maximum-over-depth sound levels from the drilling platform at White Rose Field

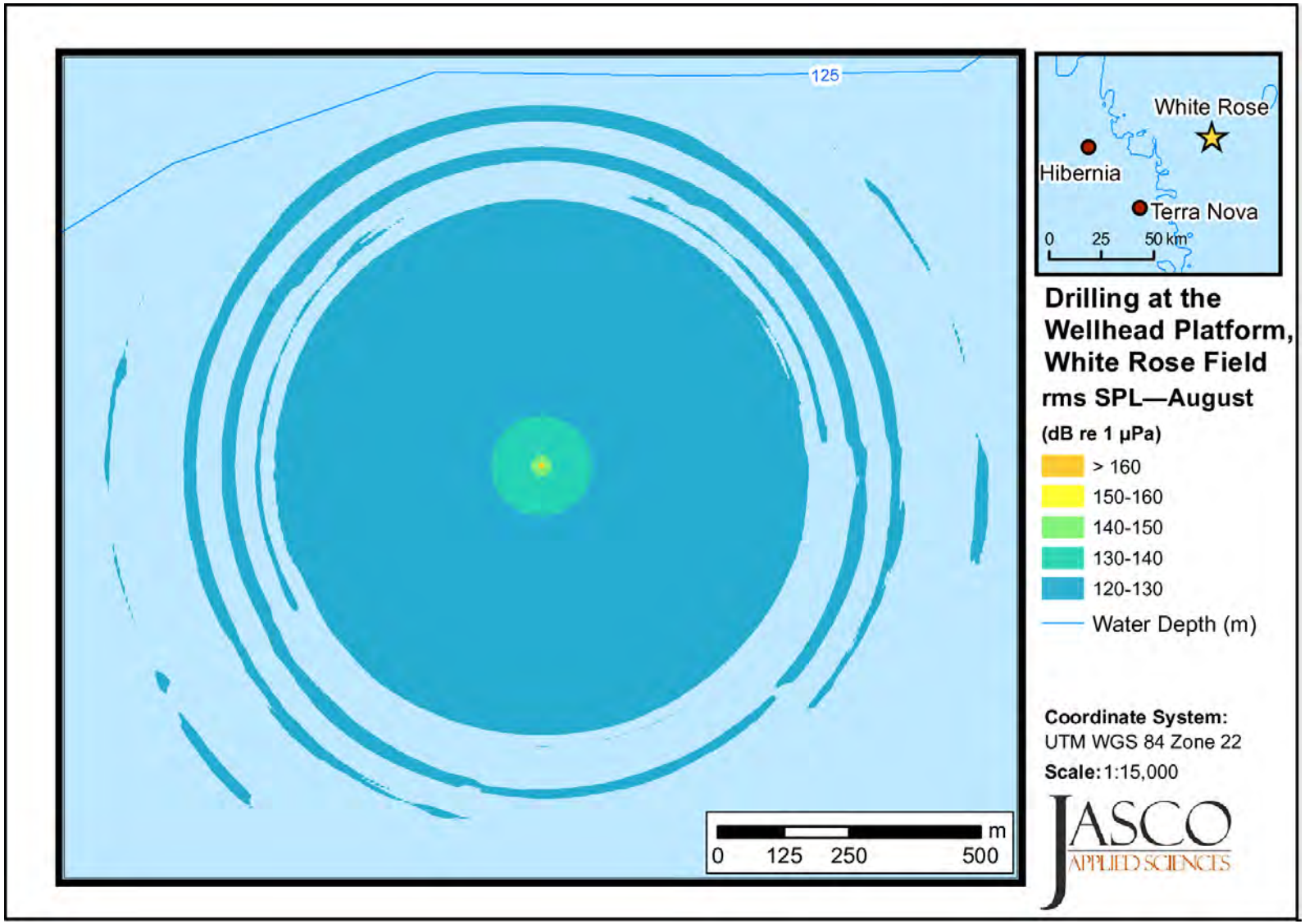

Figure 3-14 August: Received maximum-over-depth sound levels from the drilling platform at White Rose Field

3.2.3 Scenario 8: White Rose Field, Source 6 (Support Vessel)

Modelled results for Scenario 8 represent (continuous) noise from a support vessel (5 000 HP tug) operating at the White Rose field site (Tables 3-19 and 3-20; Figures 3-15 and 3-16).

Table 3-19 February: Maximum (R_{max}, m) and 95 percent ($R_{95\%}$, m) horizontal distances from the support vessel at White Rose Field to modelled maximum-over-depth sound level thresholds with and without M-weighting

rms SPL (dB re 1 µPa)	Un-weighted		LFC		MFC		HFC		Pinnipeds	
	R_{max}	$R_{95\%}$	R_{max}	$R_{95\%}$	R_{max}	$R_{95\%}$	R_{max}	$R_{95\%}$	R_{max}	$R_{95\%}$
190	—	—	—	—	—	—	—	—	—	—
180	< 5	< 5	< 5	< 5	—	—	—	—	—	—
170	7	7	7	7	< 5	< 5	< 5	< 5	< 5	< 5
160	22	22	22	22	18	18	18	18	21	21
150	83	81	83	81	65	63	63	61	75	73
140	641	528	641	526	495	365	355	303	541	487
130	4 725	3 701	4 690	3 660	4 367	2 442	3 560	2 088	4 555	3 115
120	21 800	15 650	21 800	15 598	19 483	12 986	17 204	12 026	19 553	14 427

Table 3-20 August: Maximum (R_{max}, m) and 95 percent ($R_{95\%}$, m) horizontal distances from the support vessel at White Rose Field to modelled maximum-over-depth sound level thresholds with and without M-weighting

rms SPL (dB re 1 µPa)	Un-weighted		LFC		MFC		HFC		Pinnipeds	
	R_{max}	$R_{95\%}$	R_{max}	$R_{95\%}$	R_{max}	$R_{95\%}$	R_{max}	$R_{95\%}$	R_{max}	$R_{95\%}$
190	—	—	—	—	—	—	—	—	—	—
180	< 5	< 5	< 5	< 5	—	—	—	—	—	—
170	7	7	7	7	< 5	< 5	< 5	< 5	< 5	< 5
160	22	22	22	22	18	18	18	18	22	22
150	81	79	81	79	64	62	61	60	73	71
140	600	533	600	532	536	437	440	378	552	517
130	5 155	3 567	5 155	3 546	4 431	2 882	3 374	2 554	5 036	3 215
120	19 927	13 759	19 927	13 730	16 356	11 877	15 219	11 007	19 040	13 064

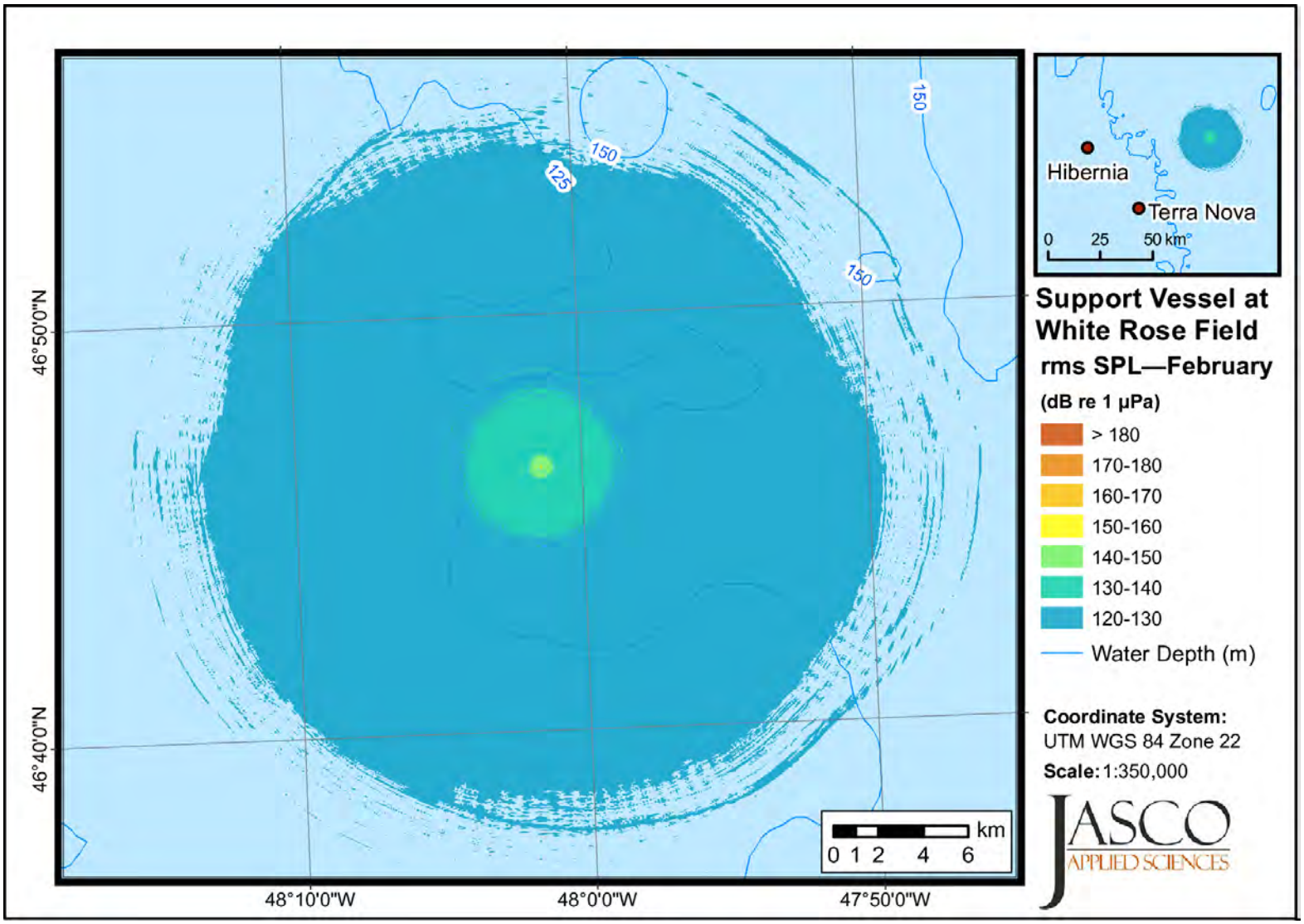

Figure 3-15 February: Received maximum-over-depth sound levels from the support vessel at White Rose Field

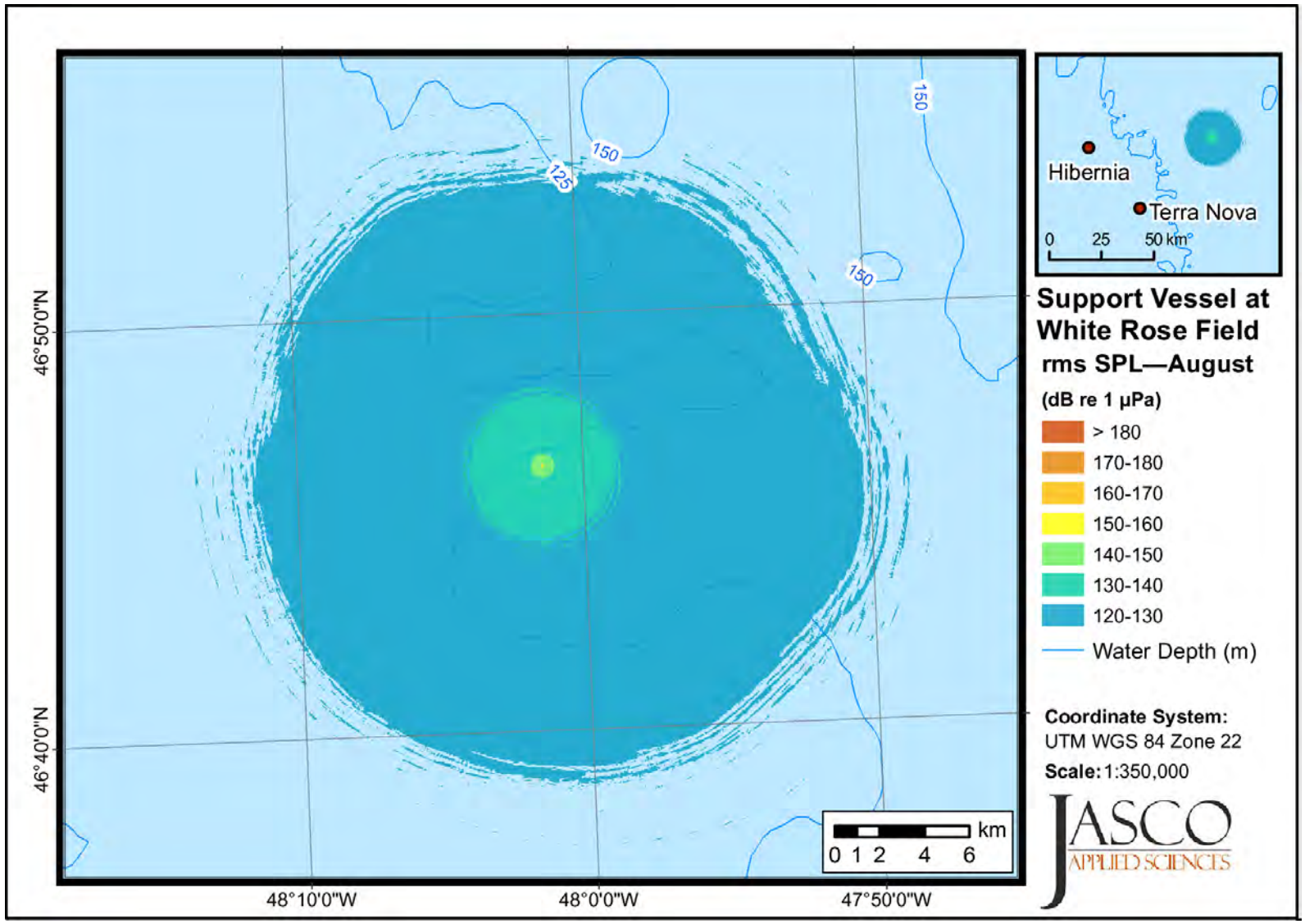

Figure 3-16 August: Received maximum-over-depth sound levels from the support vessel at White Rose Field

3.2.4 Scenario 9: White Rose Field, Source 7 (Helicopter)

Underwater received sound levels around a helicopter at an altitude of 91 m (300 ft) were estimated using the source levels from a Bell 206 helicopter and Young's (1973) model. Broadband received levels no higher than 157 dB re 1 µPa are estimated at 3 m below the surface, directly under the source, and broadband received levels no higher than 120 dB re 1 µPa, at a lateral distance of 61 m from the source (Table 3-21). Since the threshold of the 120 dB re 1 µPa rms SPL is reached at a lateral distance of less than half the water depth (128 m), distances to received sound level thresholds of 130 to 150 dB re 1 µPa were estimated assuming spherical spreading.

Table 3-21 Maximum (R_{max}, m) and 95 percent ($R_{95\%}$, m) horizontal distances from directly under the helicopter at White Rose Field to modelled maximum-over-depth sound level thresholds without M-weighting

rms SPL (dB re 1 µPa)	Un-weighted	
	R_{max}	$R_{95\%}$
170	—	—
160	< 3	< 3
150	6	6
140	10	10
130	26	26
120	61	61

The distances to the sound level thresholds are expected to vary by less than 1 m between the months. At short distances from the source (less than half the water depth (i.e., < 64 m)), M-weighting is not expected to substantially affect distances to sound level thresholds.

4.0 References

Abid, I.A., R. Hesse, and J.D. Harper. 2004. Variation in mixed-layer illite/smectite diagenesis in the rift and post-rift sediments of the Jeanne D'Arc Basin, Grand Banks, offshore Newfoundland, Canada. *Can. J. Earth Sci.* 41:401–429.

Aerts, L., M. Blees, S. Blackwell, C. Greene, K. Kim, D. Hannay, and M. Austin. 2008. *Marine mammal monitoring and mitigation during BP Liberty OBC seismic survey in Foggy Island Bay, Beaufort Sea, July-August 2008: 90-day report.* LGL Rep. P1011-1. Prepared by LGL Alaska Research Associates Inc., LGL Ltd., Greeneridge Sciences Inc. and JASCO Applied Sciences Ltd. for BP Exploration Alaska.

Blackwell, S.B., C.R. Greene, Jr, and W.J. Richardson. 2004. Drilling and operational sounds from an oil production island in the ice-covered Beaufort Sea. *J. Acoust. Soc. Am.* 116(5): 3199-3211.

Blackwell, S.B., R.G. Norman, C.R.G. Jr., and W.J. Richardson. 2007. *Acoustic measurements. Marine mammal monitoring and mitigation during open water seismic exploration by Shell Offshore Inc. in the Chukchi and Beaufort Seas, July–September 2006: 90-day report. LGL Rep. P891-1*from LGL Alaska Res. Assoc. Inc., Anchorage, AK, and Greeneridge Sciences Inc., Santa Barbara, CA, for Shell Offshore Inc., Houston, TX, Nat. Mar. Fish. Serv., Silver Spring, MD, and U.S. Fish & Wildl. Serv., Anchorage, AK. 4-1 to 4-52 p.

Buckingham, M.J. 2005. Compressional and shear wave properties of marine sediments: Comparisons between theory and data. *J. Acoust. Soc. Am.* 117(1):137-152.

Canadian Hydrographic Services. 2012. *S-57 ENC Charts: CA376135, CA376173, CA476079, CA476300, CA476805, and CA476806*.

Catto, N.R., M.R. Anderson, D.A. Scruton, and U.P. Williams. 1997. *Coastal Classification of the Placentia Bay Shore*. CAnadian Technical Report of Fisheries and Aquatic Sciences No. 2186. 58 p.

Collins, M.D. 1993. The split-step Padé solution for the parabolic equation method. *J. Acoust. Soc. Am.* 93:1736-1742.

Collis, J.M., W.L. Siegmann, M.D. Collins, H.J. Simpson, and R.J. Soukup. 2007. Comparison of simulations and data from a seismo-acoustic tank experiment. *J. Acoust. Soc. Am.* 122:pp. 1987-1993.

Coppens, A.B. 1981. Simple equations for the speed of sound in Neptunian waters. *J. Acoust. Soc. Am.* 69:862-863.

Divins, D.L. 2010. *NGDC Total Sediment Thickness of the World's Oceans & Marginal Seas* (webpage). ArcGIS files 2010. http://www.ngdc.noaa.gov/mgg/sedthick/sedthick.html.

Ellis, D. and S. Hughes. 1989. Estimates of sediment properties for ARPS. Dartmouth, Nova Scotia, Canada, 12 July 1989.

Fisher, F.H. and V.P. Simmons. 1977. Absorption of sound in sea water. *J. Acoust. Soc. Am.* 62:558-564.

Funk, D., D. Hannay, D. Ireland, R. Rodrigues, and W. Koski. 2008. *Marine mammal monitoring and mitigation during open water seismic exploration by Shell Offshore Inc. in the Chukchi and Beaufort Seas, July–November 2007: 90-day report.* LGL Rep. P969-1. Prepared by LGL Alaska Research Associates Inc., LGL Ltd., and JASCO Research Ltd. for Shell Offshore Inc, Nat. Mar. Fish. Serv., and U.S. Fish and Wild. Serv. 218, plus appendices. p.

Gales, R.S. 1982. *Effects of Noise of Offshore Oil and Gas Operations on Marine Mammals – An Introductory Assessment*. NOSC TR 844. U.S. Naval Ocean Systems Cent., San Diego, CA. NTIS AD-A123699.

Greene, C.R., Jr. 1985. Characteristics of waterborne industrial noise, 1980-84. *In:* Richardson, W.J. (ed.). *Behavior, disturbance responses and distribution of bowhead whales*

Balaena mysticetus in the eastern Beaufort Sea, 1980-84. OCS Study MMS 85-0034. Rep. from LGL Ecol. Res. Assoc. Inc., Bryan, TX, for U.S. Minerals Manage. Serv., Reston, VA. pp 197-253.

Greene, C.R., Jr 1997. *Physical acoustics measurements*. *In*: Richardson, W.J. (ed.)Northstar Marine Mammal Monitoring Program, 1996: Marine Mammal and Acoustical Monitoring of a Seismic Program in the Alaskan Beaufort Sea. LGL Rep. 2121-2. Report from LGL Ltd., King City, ON, and Greeneridge Sciences Inc., Santa Barbara, CA, for BP Explor. (Alaska) Inc., Anchorage, AK, and Nat. Mar. Fish. Serv., Anchorage, AK, and Silver Spring, MD, pp. 3-1 to 3-63.

Halliday, J. 2012. *Surficial Geology in vicinity of Placentia Bay Dredge Sites*. C-CORE Technical Memorandum, Proj. No. 270792, Doc. No. PR01. 7 p.

Halliday, J. and A. Cuff. 2012. *Argentia Acoustic Seabed Survey*. C-CORE Technical Memorandum, Proj. No. 270792. 29 p.

Hamilton, E.L. 1980. Geoacoustic modeling of the sea floor. *J. Acoust. Soc. Am.* 68:1313-1340.

Hannay, D., A.O. MacGillivray, M. Laurinolli, and R. Racca. 2004. *Sakhalin Energy – Source Level Measurements from 2004 Acoustics Programme*. JASCO Research Ltd, Victoria, BC.

Hannay, D.E. and R. Racca. 2005. *Acoustic Model Validation*. 0000-S-90-04-T-7006-00-E. Technical report prepared for Sakhalin Energy Investment Company by JASCO Research Ltd. http://www.sakhalinenergy.com/en/documents/doc_33_jasco.pdf.

Hyde, D.W. 1988. *User's guide for microcomputer programs ConWep and FunPro applications of TM 5-855-1*. *Fundamentals of protective design for conventional wepons*.

Ireland, D.S., R. Rodrigues, D. Funk, W. Koski, and D. Hannay. 2009. *Marine mammal monitoring and mitigation during open water seismic exploration by Shell Offshore Inc. in the Chukchi and Beaufort Seas, July–October 2008: 90-day report.* LGL Rep. P1049-1. Prepared by LGL Alaska Research Associates Inc., LGL Ltd., and JASCO Applied Sciences Ltd. for Shell Offshore Inc, Nat. Mar. Fish. Serv., and U.S. Fish and Wild. Serv. 277, plus appendices. p.

King, E.L. and G.V. Sonnichsen. 2000. *New insight into glaciations and sea-level fluctuation on the northern Grand Banks, offshore Newfoundland*. Geological Survey of Canada, Current Research 2000-D6. 10 p.

Lubard, S.C. and P.M. Hurdle. 1976. Experimental investigation of acoustic tranmission form air into a rough ocea. *J. Acoust. Soc. Am.* 60(5):1048–1052.

MacGillivray, A.O., M. Zykov, and D.E. Hannay. 2007. *Chapter 3: Summary of Noise Assessment; in Marine Mammal Monitoring and Mitigation During Open Water Seismic Exploration by ConocoPhillips Alaska, Inc. in the Chukchi Sea July-October 2006*. Report by LGL Alaska Research Associates and JASCO Research Ltd.

Malme, C.I., P.W. Smith, and P.R. Miles. 1986. *Characterisation of Geophysical Acoustic Survey Sounds*. Prepared by BBN Laboratories Inc., Cambridge, for Battelle Memorial Institute to the Minerals Management Service, Pacific Outer Continental Shelf Region, Los Angeles, CA.

Malme, C.I., P.R. Miles, G.W. Miller, W.J. Richardson, D.G. Roseneau, D.H. Thomson, and C.R. Greene. 1989. *Analysis and ranking of the acoustic disturbance potential of petroleum industry activities and other sources of noise in the environment of marine mammals in Alaska*. BBN Systems and Technologies Corporation for Minerals Management Service U.S. Department of the Interior.

Marine Mammal Protection Act [MMPA]. *Marine Mammal Protection Act of 1972, amended Sections 3, 101, and 104, 2004; and amended Sections 107 and 501-509 (Title V). 2007* (webpage) 2007. http://www.nmfs.noaa.gov/pr/laws/mmpa/text.htm

Matthews, M.-N.R., M. Zykov, and T. Deveau. 2010. *Assessment of Underwater Noise for the Mary River Iron Mine: Construction and Operation of the Steensby Inlet Port Facility*. Technical report prepared for LGL Limited (King City) by JASCO Applied Sciences.

McCauley, R.D., M.-N. Jenner, C. Jenner, K.A. McCabe, and J. Murdoch. 1998. The response of humpback whales (*Megaptera novaeangliae*) to offshore seismic survey noise: preliminary results of observations about a working seismic vessel and experimental exposures. *Austral. Petrol. Prod. & Explor. Assoc. J.* 38:692-707.

Mosher, D.C. and G.V. Sonnichsen. 1992. *Stratigraphy and Sedimentology of sediments on the northeastern Grand Banks of Newfoundland from borehole investigation*. Geological Survey of Canada, Open File 2409. 110 p.

Nedwell, J.R. and A.W. Turnpenny. 1998. *The use of a generic frequency weighting scale in estimating environmental effect. . Workshop on Seismics and Marine Mammals* 23–25th June, London, U.K.

Nedwell, J.R., A.W.H. Turnpenny, J. Lovell, S.J. Parvin, R. Workman, J.A.L. Spinks, and D. Howell. 2007. *A validation of the dB_{ht} as a measure of the behavioural and auditory effects of underwater noise*. 534R1231 prepared by Subacoustech Ltd for the U.K. Department of Business, Enterprise and Regulatory Reform under Project No. RDCZ/011/0004.

NMFS. 2005. *Endangered Fish and Wildlife; Notice of Intent to Prepare an Environmental Impact Statement.*

O'Neill, C., D. Leary, and A. McCrodan. 2010. *Sound Source Verification. (Chapter 3) In Blees, M.K., K.G. Hartin, D.S. Ireland, and D. Hannay. (eds.) Marine mammal monitoring and mitigation during open water seismic exploration by Statoil USA E&P Inc. in the Chukchi Sea, August–October 2010: 90-day report.* LGL Report P1119. Prepared by LGL Alaska Research Associates Inc., LGL Ltd., and JASCO Applied Sciences Ltd. for Statoil USA E&P Inc., Nat. Mar. Fish. Serv., and U.S. Fish and Wild. Serv. 3-1, 3-34 p.

Osler, J. 1994. *A geo-acoustic and oceanographic description of several shallow water experimental sites on the Scotian Shelf*. Technical Memorandum 94/216. DREA, Dartmouth, Nova Scotia, Canada. pp Measurements. pp. 47 p.

Porter, M. and Y.C. Liu. 1994. *Finite-element ray tracing. in Proceedings of the International Conference on Theoretical and Computational Acoustics*. Volume 2, Singapore.

Richardson, W.J. and C.I. Malme. 1993. Man-made noise and behavioral responses. . *In:* Burnes, J.J., J.J. Montague, and C.J. Cowles (eds.). *The bowhead whale.* . Spec. Publi. 2 Soc. Mar. Mammal., Lawrence, KS. . pp 631-700.

Richardson, W.J., C.R. Greene, Jr, C.I. Malme, and D.H. Thomson. 1995. *Marine Mammals and Noise.* . Academic Press, San Diego, California. 579 p.

Robinson, S.P., P.D. Theobald, G. Hayman, L.S. Wang, P.A. Lepper, V. Humphrey, and S. Mumford. 2011. *Measurement of noise arising from marine aggregate dredging operations*. MALSF (MEPF Ref no. 09/P108).

Rodriguez, E., C.S. Morris, Y.J.E. Belz, E.C. Chapin, J.M. Martin, W. Daffer, and S. Hensley. 2005. *An assessment of the SRTM topographic products.* . JPL D-31639. Jet Propulsion Laboratory Pasadena, CA.

Southall, B.L., A.E. Bowles, W.T. Ellison, J.J. Finneran, R.L. Gentry, C.R.G. Jr., D. Kastak, and D.R. Ketten. 2007. Marine mammal noise exposure criteria: Initial scientific recommendations. *Aquatic Mammals* 33:411–521.

Teague, W.J., M.J. Carron, and P.J. Hogan. 1990. A comparison between the Generalized Digital Environmental Model and Levitus climatologies. *J. Geophys. Res.* 95(C5):7167-7183.

TM 5-855-1. 1986. *Fundamentals of Protective Design for Conventional Weapons, US Army Waterways Experimental Station*. US Army.

Urick, R.J. 1972. Noise Signature of Aircraft in Level Flight over and Hydrophone in the Sea. *J. Acoust. Soc. Am.* 52:993.

Warner, G., C. Erbe, and D. Hannay. 2010. *Underwater sound measurements. (Chapter 3) In: Reiser, C. M, D. W. Funk, Rodrigues, and D. Hannay. (eds.) Marine mammal monitoring and mitigation during open water seismic exploration by Shell Offshore, Inc. in the Alaskan Chukchi Sea, July–October 2009: 90-day report.* LGL Report P1112-1. LGL Alaska Research Associates Inc. and JASCO Applied Sciences Ltd. for Shell Offshore Inc, Nat. Mar. Fish. Serv., and U.S. Fish and Wild. Serv. 3-1, 3-54 p.

Young, R.W. 1973. Sound Pressure in water from a source in air and vice versa. *J. Acoust. Soc. Am.* 53(6):1708–1716.

Zykov, M., A.O. MacGillivray, M. Austin, O. McHugh, B. Wheeler, and M. Fraker. 2007. *Source Level Study of the Dredge Columbia and Killer Whale Acoustics Impact Report Update* by Jacques Whitford – AXYS and JASCO Research Ltd. for Vancouver Port Authority.

Zykov, M., T. Deveau, and D. Hannay. 2010. *Underwater pressure measurements of blasting in a river environment*. Upublished report by JASCO Applied Sciences.

5.0 Acronyms

Term	Description
BHP	break-horsepower
CGS	concrete gravity structure
ConWep	Conventional Weapons Effects Software
CSD	cutter suction dredge
FWRAM	Full-Waveform Acoustic Propagation Model (based on RAM)
GDEM	Generalized Digital Environmental Model
HFC	high-frequency cetacean functional hearing group
LFC	low-frequency cetacean functional hearing group
MFC	mid-frequency cetacean functional hearing group
MONM	Marine Operations Noise Model
MOODS	Master Oceanographic Observational Data Set
M-weighting	marine mammal frequency weighting
NMFS	(United States) National Marine Fisheries Service
PE	parabolic equation
RAM	Range-dependent Acoustic Model
RAM-S	Range-dependent Acoustic Model with Shear Waves
rms SPL	root-mean-square sound pressure level
SEL	sound exposure level
SPL	sound pressure level
THP	total horsepower
TNT	trinitrotoluene
TSHD	trailing suction hopper dredge
UTM	Universal Transverse Mercator
WHP	wellhead platform
WREP	White Rose Extension Project